Similar striatal activity exerts different control over automatic and flexible motor sequences

Kevin G. C. Mizes[1,3], Jack Lindsey[2], G. Sean Escola[2] and Bence P. Ölveczky[3]

1. Program in Biophysics, Harvard University, Cambridge, MA 02138, USA.
2. Zuckerman Mind Brain and Behavior Institute, Columbia University, New York, NY, 10027, USA
3. Department of Organismic and Evolutionary Biology and Center for Brain Science, Harvard University, Cambridge, MA, USA

Abstract

The ability to sequence discrete movements in new ways enables rich and adaptive behavior. Such flexibility can be computationally costly and result in halting performances. Practicing the same motor sequence repeatedly, however, can render its execution precise, fast, and effortless, i.e., 'automatic'. The basal ganglia are thought to underlie both flexible and automatic motor sequences, yet how their contributions differ across these modes is unclear. We parse this in rats trained to perform the same motor sequence in both modes, focusing on the sensorimotor striatum. Neural recordings revealed a kinematic code independent of execution mode. While lesions affected the detailed kinematics across modes, they disrupted high-level sequential structure for automatic but not visually-guided flexible behaviors. These results suggest that while the basal ganglia contribute to learned movement kinematics and are essential for 'automatic 'motor skills, they can be dispensable for the flexible sequencing of discrete motor elements.

Introduction

Our ability to sequence movements and actions in response to new and unpredictable challenges allows us to imitate trendy dance moves or play Chopin etudes from sheet music. Assembling motor sequences in such flexible ways can be mentally taxing and computationally costly, resulting in slow[1] and error-prone performances subject to cognitive interference[2,3]. Repeatedly executing the same motor sequence, such as typing a password or practicing a favorite piano sonata, yield continuous task-specific movement patterns that are fluid and fast[4–7], precise[5], efficient[8], and less cognitively demanding[2,9,10]; in a word: 'automatic'[11–13]. In contrast to flexible motor sequences[3], which are informed by sensory cues and/or memory-guided decision-making processes[14], automatic motor sequences can be specified and stored as sequential low-level motor commands[15–17].

Given the differences in how flexible and automatic motor sequences can be specified and the computational demands associated with their execution, the neural circuits underlying them are thought to differ[10,14,18–23]. Our colloquial reference to automatic motor sequences as being stored in 'muscle memory' reflects a subjective sense that they are, in contrast to flexible cognitive behaviors, less reliant on cognitive processes and controlled by circuits closer to the motor periphery[11,18,21,24]. Yet, despite a consensus that automatic and flexible behaviors engage different neural substrates, the specifics of these are not well understood[14,25–27].

The basal ganglia (BG), a set of motor-related midbrain nuclei whose output modulate both cortical and subcortical control circuits[28], have been implicated in various aspects of motor sequence learning and execution[20,24,29–32]. Importantly, the relevant computations and control functions ascribed to the BG and thought to be elaborated across their sensorimotor and associative regions[33], contribute to flexible and automatic behaviors in different ways and to different degrees[18,21,34–36].

Because flexible motor sequences can be equated to serial action selection or decision making[26,37], it follows from BG's acknowledged role in these processes[20,32,38,39] that they should be central to flexible motor sequencing. While recordings showing sequence-specific neural activity in the primate and human BG are consistent with this view[40,41], more recent studies have called this into question. For example, inactivating a main output nucleus of the BG (GPi) in monkeys did not affect their ability to generate visually guided reaching sequences beyond reducing the speed and/or amplitude of the constituent movements[42].

Some of the discrepancy across studies may be due to flexible motor sequences being generated, and hence probed, in different ways. For example, they can be guided by sensory cues (externally guided) or from working memory (internally guided)[14,43]. Recordings from GPi neurons in monkeys performing the same sequences in the two modes revealed more task-modulated neurons in working memory trials[44], implying that the BG may be engaged to a greater degree in flexible motor sequences if they are informed by working memory, a notion supported also by studies in humans[45].

Automaticity, on the other hand, is distinguished by stereotypy and lack of flexibility. Once an 'automatic' motor sequence has been initiated, there are no major decision points and, hence, no need for discrete action selection. Studies showing neural activity in sensorimotor regions of the BG preferentially encoding the start and stop of overtrained behaviors[46–50] imply that repeated practice may transform discrete motor sequences – with distinct elements and choice points – into immutable continuous sequential movement patterns[1,12]. While sensorimotor regions of the BG are thought to help select and initiate such 'chunked' behaviors[51,52], the implication of these studies is that their detailed progression and specification are elaborated in downstream control circuits.

The generality of this view, however, has been challenged by recent studies showing that the BG is necessary for specifying and generating the detailed kinematics of stereotyped learned behaviors[15,53–56]. In these studies, the activity patterns in the sensorimotor striatum did not reflect the starts and stops of the overtrained behaviors, nor specific choice points in the sequences; rather, the neurons encoded the kinematic details of the sequential behaviors, suggesting an essential role for the BG in the low-level kinematic specification of automatic movements.

To directly address the role of the BG in motor sequence execution and how it may differ across execution modes, we designed a paradigm in which rats are trained to execute the same three-element motor sequence in both flexible and automatic (i.e. overtrained) contexts[57]. Surprisingly, neural recordings in the sensorimotor arm of the striatum (dorsolateral striatum, DLS, in rodents) – a region implicated in behavioral automaticity[33] – revealed no meaningful difference across execution modes with neurons representing low-level kinematic features for both flexible and automatic motor sequences. The neural population showed no selectivity for higher-level attributes of the behavior, such as the order or sequential context of a given movement. Lesions to the DLS, however, revealed a stark contrast across modes of execution, with sequence organization being essentially lost for automatic sequences but largely preserved when the same sequence was guided by visual cues. Additionally, lesions rendered the movements across both modes slower and more variable, resembling the animal's engagement with the task early in learning, a finding consistent with a general role for the BG in specifying learned kinematics[15]. Lesion of the associative arm of the striatum (dorsomedial striatum in rodent; DMS), widely implicated in behavioral flexibility[58–62], did not affect performance or motor execution in any mode.

A simple network model simulating DLS and its interactions with other motor circuits could recapitulate these results, including the differing impacts of DLS lesions on flexible and automatic sequences and a role for DLS in the kinematic specification across execution modes.

Results

A discrete sequence production task for rats

To directly compare the neural substrates of flexible and automatic motor sequence execution, we designed a discrete sequence production task for rats based on similar paradigms in humans and non-human primates (NHPs)[22,57,63]. Importantly, we wanted our paradigm to distinguish motor automaticity from habit formation[11,12], two independent processes that can occur alongside each other and that may involve some of the same neural substrates[11,64,65]. Thus, we designed our task to ensure that rats achieve automaticity on a motor sequence without developing it into a habit. Since habits tend to form when the correlation between actions and outcomes is weak or variable[66–68], if the reward is delayed[69], or, further, if the reward is appetitive or addictive[70–72], our paradigm directly linked behavioral variants to a water reward in a training process[68] that resulted in highly overtrained behaviors expressed in goal-directed ways (Extended Data Fig. 1).

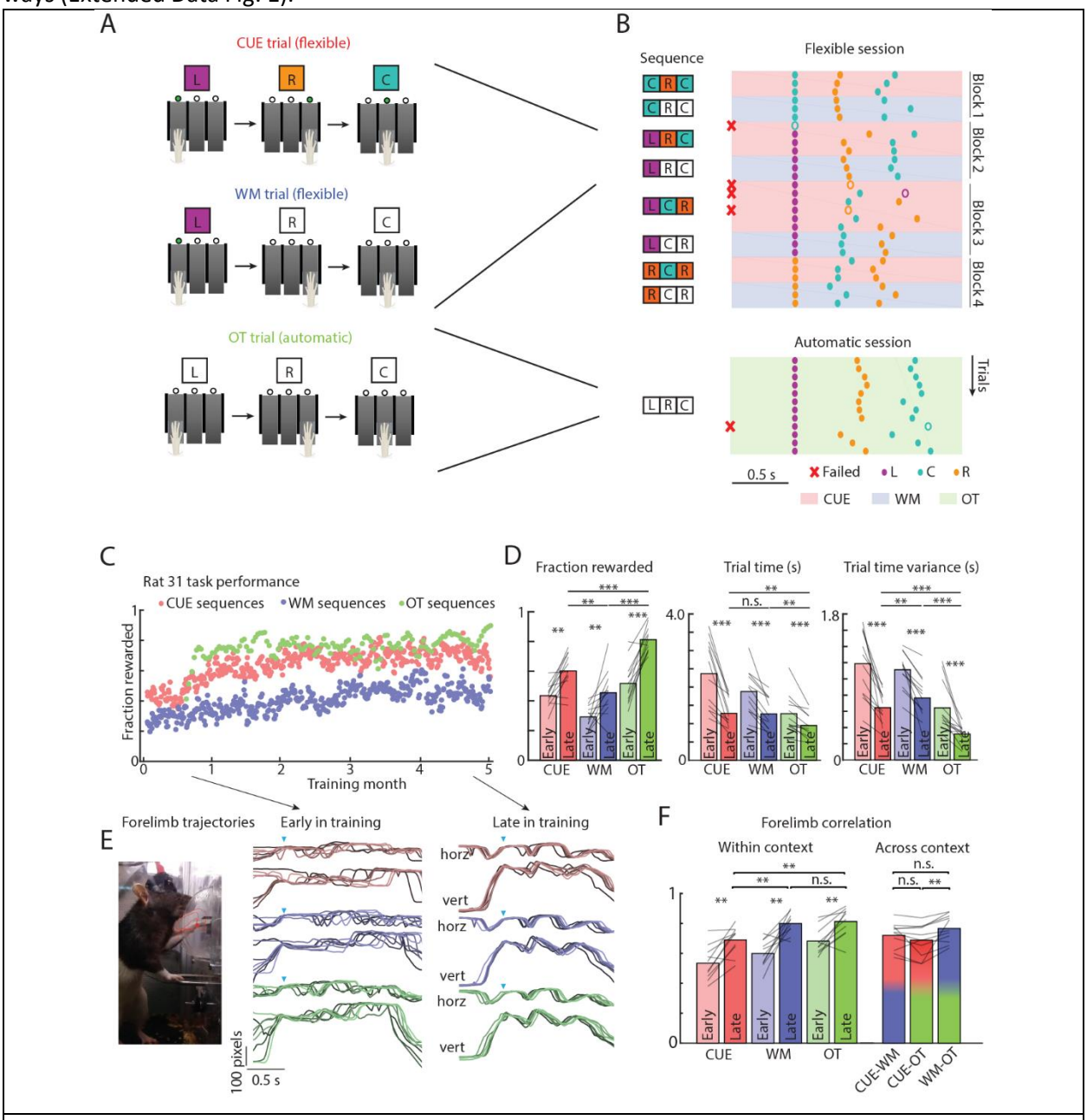

Figure 1: Paradigm for training rats to produce flexible and automatic motor sequences

A. Rats learn to generate 3-element lever-press sequences that, in 'flexible' training sessions, are either visually cued (CUE) or generated from working memory (WM) by repeating the sequence from the preceding cued trial. In a separate 'automatic' session without any cues, the same sequence is rewarded each day. **B.** Performance of an example rat in a flexible session (top) and automatic session (bottom). In flexible sessions, sequences are randomly chosen, from 12 possible sequences, and change every block. **C.** Fraction of rewarded trials per session in the three execution modes (red=CUE, blue = WM, green = OT) for one animal over several months of training. **D.** Fraction of rewarded trials (left), trial time (middle) and variance in trial time (right), improve from early (light color) to late (dark color) in training across all three execution modes (n=12 rats). **E.** Forelimb trajectories, aligned to the first lever press, for 8 example trials from early and late in learning. Examples selected from trials with similar duration. **F.** Trial-to-trial correlation of the active forelimb trajectory within a given execution mode from early and late in training (n=10 of 12 rats were tracked in early learning), and correlation of the kinematics across the three modes, late in training. *P<0.05, **P<0.01, ***P<0.001, Wilcoxon sign rank test.

Specifically, we trained rats to sequence readily expressed movements and actions in prescribed ways. To facilitate comparisons to other motor-related studies in rodents, including our own[15,16], which probe forelimb[29,32,48,50,55,73] and whole-body orienting[74–76] movements, we opted for a 'piano-playing' task, in which rats are rewarded for performing sequences of three keypresses on a three-key 'piano' in a prescribed order alternating between forelimb lever-presses and orienting movements (12 possible sequences; see Fig. 1a, Supplementary Movie 1).

Rats were initially trained to press a single lever for a water reward, then to associate a visual cue above each lever with pressing that lever (see Methods). After acquiring the cue-action association for each of the levers (5164 ± 948 trials; mean ± s.e.m), rats transitioned from single presses to two- and, ultimately, three-element sequences. In flexible training sessions, the rewarded keypress sequence was either signaled directly by visual cues (**CUE**) or had to be remembered from the instructed sequence of previous trials (working memory, **WM**) (see Methods). This trial design, adopted from studies in NHPs[43], allowed us to compare performance and neural dynamics for flexible sequences guided by visual cues and those generated from working memory[22,23,77–79]. Blocks of CUE and WM trials were interleaved and, in each, one of the 12 possible sequences was randomly selected and rewarded (Fig. 1b).

In separate automatic training sessions (see Methods), animals were rewarded for producing the same pre-determined keypress sequence for the duration of the months-long experiment (overtrained mode, **OT**). Because this is one of the 12 sequences rewarded in the flexible session, we could compare the same sequence across execution modes.

Rats master the 'piano playing' task

Rats learned to produce the prescribed sequence under all three conditions (CUE, WM, OT) (Fig. 1c-d). We deemed rats to be 'experts' when both their success rates and trial times were reliably within 0.5 σ of asymptotic performance values (see Methods). Expert performance was reached after 17,623 ± 7616 trials (75 ± 23 days) in the CUE mode, 11330 ± 5278 trials (88±30) days in the WM mode, and 14061 ± 7082 (72 ± 21 days) trials in the OT mode.

The success rate of expert rats was, on an average, 60.19% ± 10.73% (CUE), 44.29 ± 15.45% (WM) and 79.57 ± 11.84% (OT). Note that in all cases, this is many times chance performance, which would be 8.33% considering only the 12 prescribed sequences or 3.7% considering all possible three element keypress sequences. As is expected from similar learning paradigms in humans and NHPs[6,7,22], the mean and variability of the trial times decreased with learning (Fig. 1d), while the stereotypy and the smoothness of the associated movement patterns increased across all three execution modes (Fig. 1e-f, Extended Data Fig. 2).

Kinematic similarities across execution modes and movement elements

Probing a distinction in how neural circuits implement flexible and automatic motor sequences requires dissociating differences in execution mode from differences in movement kinematics. To establish the degree to which kinematics for the same motor sequence across session types (i.e. CUE, WM or OT) were similar, we tracked the rat's dominant forelimb (i.e. the one pressing the lever) in recorded videos (Fig. 1e, Supp vid 1) [80,81]. Comparing trials of similar duration across session types revealed very similar forelimb trajectories. Pairwise correlations – of trajectories linearly warped to lever press times – had similar distributions whether the trials were from within or across session types (Fig. 1f). This is important because it allows us to interpret any potential differences in neural activity and sensitivity to neural manipulations across session types as being due to differences in execution mode (OT, WM, CUE) rather than in the overall structure of their movements.

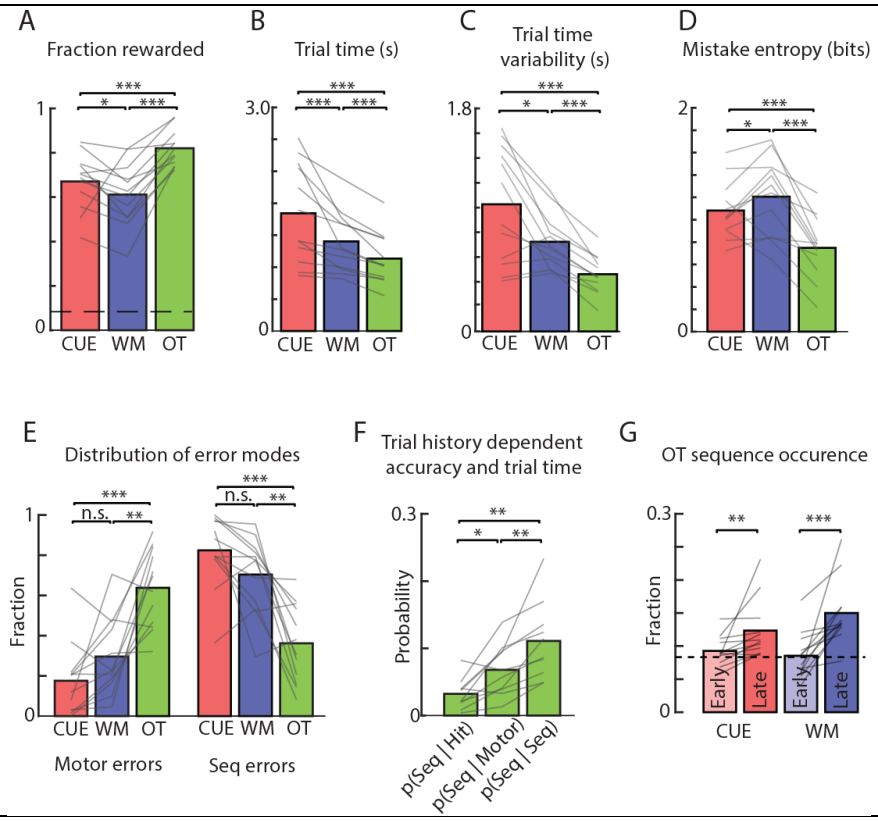

Figure 2: Overtrained motor sequences show signatures of automaticity.
A-D. Performance metrics for the same sequence across execution modes. Gray lines are averages within rats; bars are the grand average across rats. **A.** Success rate, or fraction of rewarded trials. **B.** Median trial duration for rewarded sequences measured as the time from the 1st to the 3rd lever press. **C.** Standard deviation of trial durations. **D.** Variability, or Shannon entropy, of the mistakes made in unrewarded trials (see Methods). **E.** Fraction of unrewarded trials classified as either motor errors or sequence errors (see Supplementary Movie 2 and Methods). **F.** Probability of a sequence error, if the previous trial was rewarded (Hit), a motor error, or a sequence error (Seq), in the overtrained condition. **G**. Probability that the rat performs the overtrained sequence in the flexible session before and after the overtrained sessions are introduced. Dotted line is chance of performing any particular sequence (8.33%). *P<0.05, **P<0.01, ***P<0.001, Wilcoxon sign rank test.

Flexible and automatic motor sequence execution differ

In humans, motor automaticity is distinguished by improved performance, increased movement speed, and less variable execution times[1,11,12]. While we found that kinematics for the same motor sequence across session types was similar (Fig. 1e-f, Supplementary Movie 1), we parsed these metrics in the behavioral data to assess whether automaticity, had been established in OT sessions (Fig 2a-d).
Consistent with signatures of automaticity, we found that trials in OT sessions were more successful, faster, and less variable than in flexible sessions (Fig. 2a-c). We also examined the failure modes, hypothesizing that rats performing automatic sequences should be more systematic, or less variable, in the errors they make[82]. In agreement with this, we found that the entropy, or randomness, of the distribution of erroneous sequences was much lower in the OT sessions than for either of the flexible sessions (CUE,WM; Fig. 2d).

Furthermore, if automatic motor sequences are consolidated and defined in terms of continuous low-level motor commands[15,55,56,83], unsuccessful trials in OT sessions should be dominated by errors relating to variability in movement kinematics (e.g. a forelimb swipe at the 'correct' lever but missing the target), as opposed to errors in higher-level motor sequencing (Supplementary Movie 2) .

In support of this, failures in OT trials were mostly due to rats swiping at but missing the 'correct' lever or failing to depress it beyond the threshold for detection (approximately 63.81 ± 19.56% of all OT errors were of this type; Fig. 2e). This was in contrast to flexible trials, in which unsuccessful attempts were dominated by true sequence errors, where rats orient towards and press the 'wrong' lever (only 17.6 ± 18.25 % of CUE and 29.62 ± 19.02% of WM errors were motor errors). Interestingly, potential sequence errors in the OT sessions were twice as likely to come after trials with motor execution errors compared to correct trials (Fig. 2f, Extended Data Fig. 3, see Methods), consistent with a drop in reward triggering increased motor exploration[82].

Similar to studies in humans and NHPs performing both flexible and automatic motor sequences[4,42,84], rats were more likely to execute the overtrained sequence in flexible sessions compared to chance (12.35±4.43% in CUE, 14.99±4.85% in WM, where chance is 8.3%; Fig. 2g).

These differences in the quality of motor sequence execution and the error modes across the distinct session types are consistent with studies of flexible and automatic motor sequence execution in humans[4–7,85] and indicate that automaticity of the overtrained motor sequence, as commonly defined in the literature, had been achieved.

DLS represents automatic and flexible motor sequences similarly

We had designed our behavioral paradigm to directly probe whether and how the neural implementations of flexible and automatic motor sequences differ at the level of the BG. If the BG indeed distinguish these modes of execution, as widely believed, we argued that it should manifest as a difference in the associated neural activity patterns. To directly and effectively probe this, we implanted 64-channel tetrode drives targeting the DLS in expert rats (n=4, Extended Data Fig. 4a) and compared the activity of the same neurons for the same motor sequence in OT, CUE and WM sessions. We recorded neural activity continuously over several weeks, comparing units recorded for at least 5 trials for each execution mode (CUE, WM, OT) for the same motor sequence (in total: n=579 neurons selected from 2468 total, see Methods).

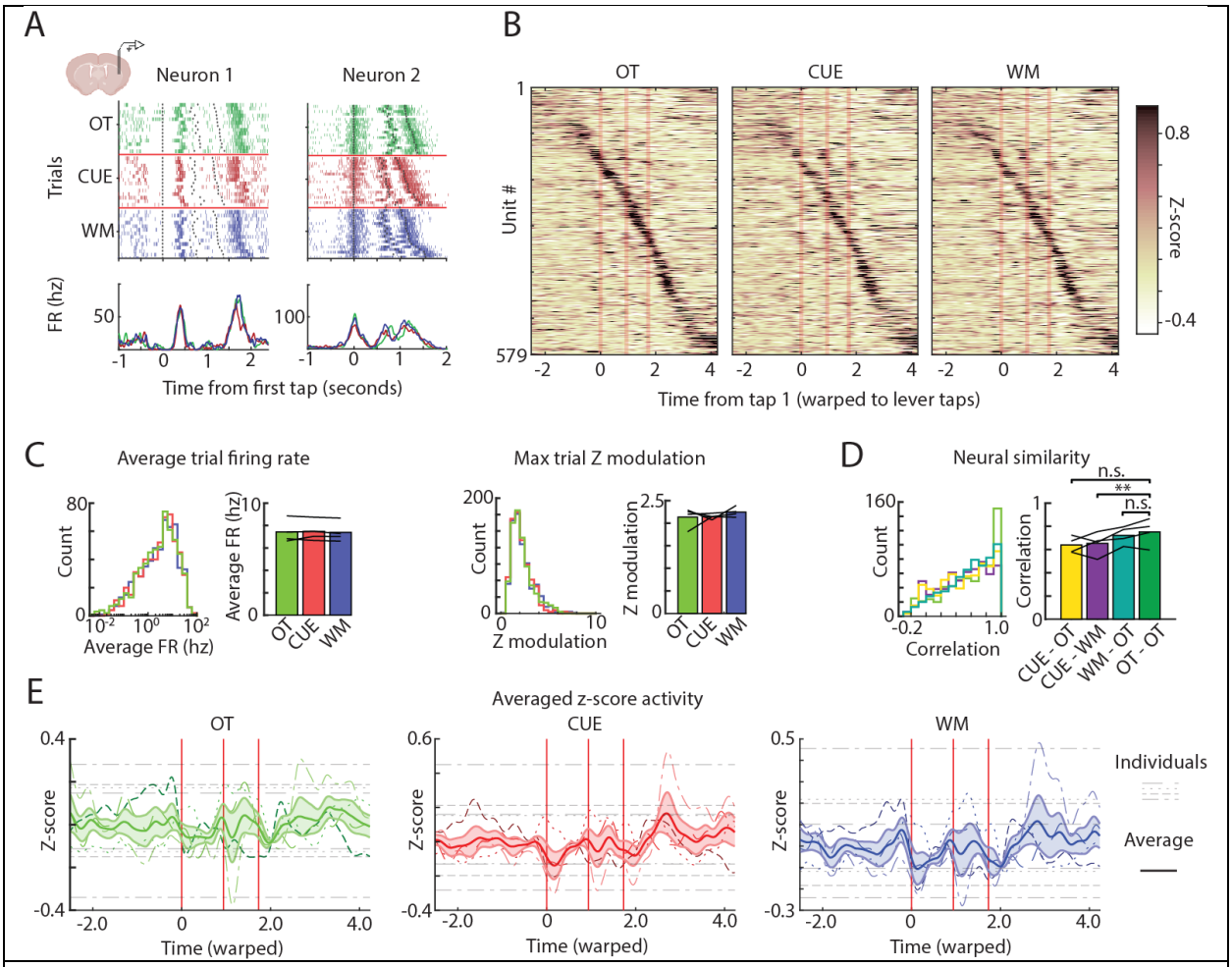

Figure 3: DLS represents automatic and flexible motor sequences similarly

A. Spike rasters for two example neurons recorded in DLS during the execution of the same motor sequence in OT (green), CUE (red), and WM (blue) execution modes. Black dots indicate the time of a lever press; red lines separate the execution modes. Below is the instantaneous firing rate across each execution mode. Trials were subsampled to have equal trial durations across execution modes. **B.** Z-scored average activity of 579 neurons recorded in the DLS for the same sequence during the OT, CUE, and WM execution mode (from n=4 rats). The trials were linearly time-warped to each lever press (red vertical lines). Units were sorted by the time of their peak activity. The sorting index was calculated from half the available trials for each unit, taken from the OT mode, and then applied to the remaining trials and modes. **C.** Comparing task-aligned activity statistics across the population of recorded neurons. (Left) Histogram of the average firing rate during the trial-period (P>0.05, paired t-test for each execution mode). The bar graph breaks this down by rats (n=4). (Right) Same as in the left panel but for maximum modulation of Z-scored firing rate during the trial-period (P=.94 OT-CUE, P=.25 OT-WM, P=.26 CUE-WM, paired t-test). **D.** Histogram of correlation coefficients between trial-averaged activity across execution modes for the DLS neurons shown in **B** (see Methods)**.** Left, histogram of the correlation coefficients of the trial-averages neural activity on CUE and OT trials (yellow), CUE and WM trials (purple), WM and OT trials (cyan), and OT and a heldout set of OT trials (green). Right, mean correlation coefficients for trial-averaged activity across execution modes broken down by animal (n=4). **P<0.01, paired t-test. **E.** *Z*-scored firing rates averaged over all neurons. Thick, solid lines indicate the grand average across all rats (n=4), and colored shaded regions indicate the s.e.m. across rats. Thin, dashed lines indicate individual rats, and the thin, dashed gray lines denote the 95% confidence interval of z-scored activity.

The comparisons across each execution mode (Fig. 3a) were striking for the lack of any qualitative difference: task-related activity patterns of DLS neurons for the same motor sequence were highly correlated across all trial types (CUE, WM and OT; Fig. 3a-b) with no significant difference in either the average firing rates or peak z-scored activity (Fig. 3c,d). Thus, the neural recordings, on their own, did not suggest a meaningful difference in how the BG, in the context of a goal-directed task, are engaged in flexible and automatic motor execution despite prior suggestions to the contrary[18,21,34–36]. Surprisingly, our recordings also did not show a clear distinction between visually and memory guided sequences[44,45].

The DLS does not encode high-level features of the sequence

We next analyzed neural activity patterns in DLS for clues about the general contributions it makes to motor sequence execution, focusing first on its putative role in discrete action selection. Prior studies supporting such a function have interpreted elevated average DLS activity at the boundaries of 'chunked' actions[46,49,50,86] as an indication that the BG help bias their initiation and/or termination by facilitating and/or inhibiting downstream control circuits[51]. To test whether activity is concentrated at the boundaries of putative action 'chunks', we examined the firing rate modulation over the length of the whole sequence (Fig. 3e; see methods). We found no evidence for population activity in the DLS preferentially marking the start and stop of overtrained sequence; neither did it, for flexible motor sequences, mark the boundaries between behavioral elements (lever presses, lever orienting movements) or pairs of such (combined orient and press movements) (Fig. 3e).

While average population activity in DLS did not demarcate the boundaries of motor elements or motor chunks, its activity could reflect their place in the sequence in other ways[40,41,87]. For example, it has been proposed that DLS neurons represent the sequential context of movements and action, including their ordinal position or, in lever pressing tasks, the identity of the lever being pressed[48,88]. In such a coding scheme DLS activity associated with a specific movement would not be a mere function of its kinematics, but also reflect higher-order features of the sequence[26].

To explicitly probe this, we expanded our analysis to all 12 motor sequences generated in flexible sessions. If DLS represents higher-order features of sequence organization, its neural activity should differ when the same lever press or orienting movement is performed in different sequential contexts (e.g., the press and orienting movement L→C in the sequence L→C→L vs. the sequence C→L→C; Fig. 4a). We did not find this to be the case: neural activity across two sequences composed of different elements (L→C→L vs. C→R→C) but similar lever press and orienting movements (press→move right→press→move left→press), was similar (Fig. 4a). More generally, DLS activity associated with a given motor element was highly correlated regardless of the sequence in which it was embedded, its ordinal position in the sequence (1st, 2nd, 3rd press), or the specific lever being pressed (i.e. L, C, or R) (Fig. 4a-e). There was however a very clear distinction in how striatal neurons represented orienting movements to the left and right, consistent with an egocentric kinematic code (Fig. 4d-e).

DLS encodes detailed movement kinematics

Based on this initial analysis and related studies[15,53,55,56], a plausible alternative to DLS representing higher-order aspects of discrete motor sequences is that is encodes - and contributes to shaping - the detailed kinematics of learned sequential movement patterns. While DLS is not required for species-typical lever-press or orienting movements[15,32,76,89], it can, by acting on downstream control circuits, help make them more adapted to the specific task[15,55,90] (Fig. 1e). In this scenario, we would expect DLS neurons to encode kinematic features continuously throughout the behavior[15,56,83].

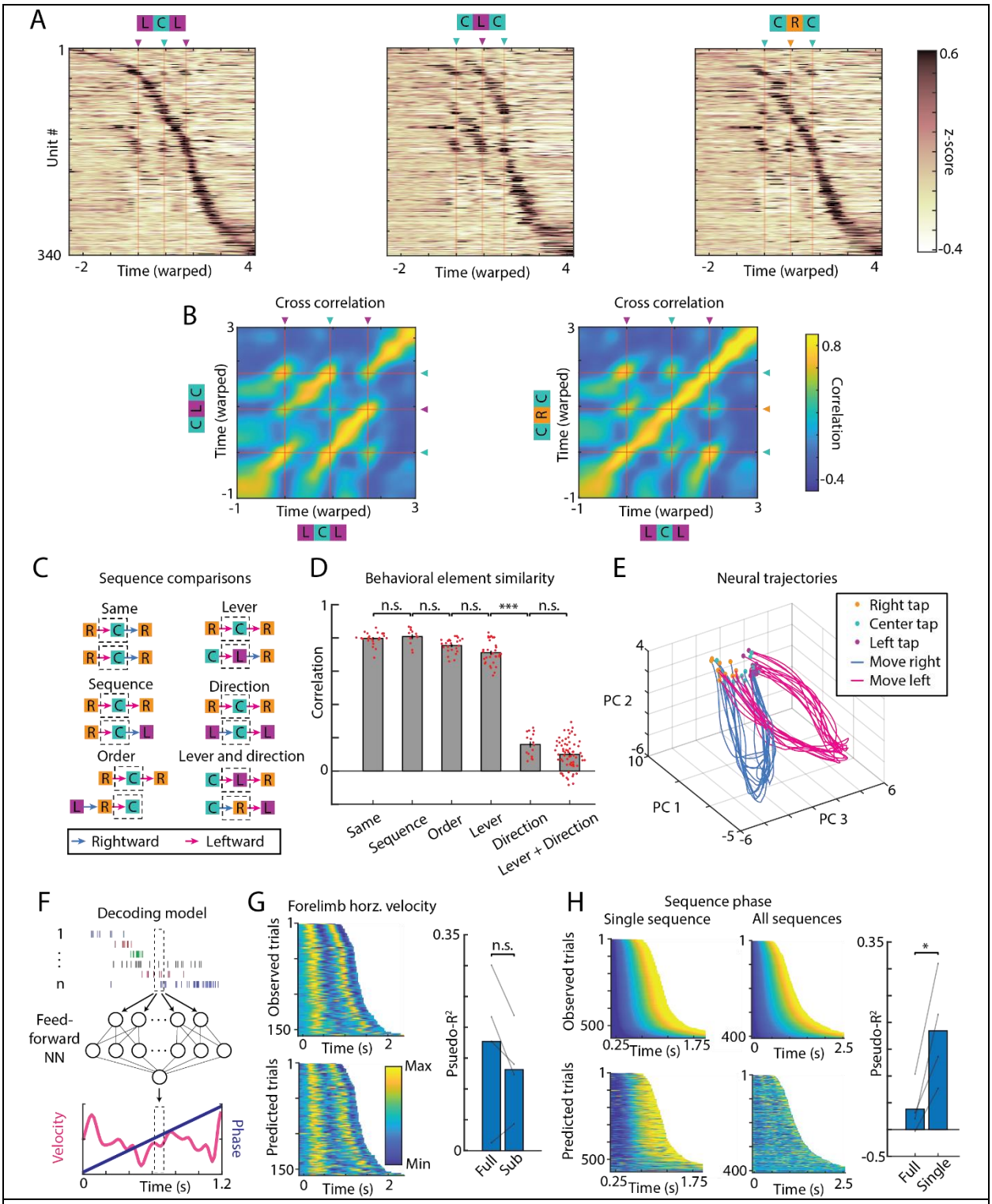

Figure 4: DLS encodes low-level kinematics, not high-level attributes, of discrete motor sequences

A. Comparing trial-averaged neural activity for different sequences, from all DLS neurons that met our criteria for inclusion (See Methods), across 4 rats. Units were sorted based on time of peak firing rate in the LCL sequence (left most). Sequences LCL and CLC (left and center), are comprised of the same motor elements (LC and CL) but ordered differently. Sequences LCL (left) and CRC (right) are comprised of the same actions (press, move right, press, move left, press), but on different levers. **B.** Cross correlations of time-varying neural activity from A (see Methods). **C.** The flexible condition allows us to compare the same sub-sequence of orienting and pressing movement (here: rightward orienting and pressing) in different sequential contexts. Dashed box indicates examples of comparisons made in D. **D.** Correlation of the neural activity patterns associated with the same sub-sequence of orienting and pressing movements in different sequential contexts. ***P<0.001, Bonferroni corrected Wilcoxon rank sum test. **E**. Neural population trajectories in PC space for the 12 different sequences, plotted along the 1st, 2nd, and 4th PC. In DLS, all lever press movements (color dots) are associated with similar neural activities, as are all right- (cyan) and left-ward (magenta) movements, independent of lever identity or order in the sequence (i.e., right→center, center→left, and right→left are all similar). **F-H**. Decoding analysis. **F**: Schematic of the decoding analysis. A feedforward neural network was trained to predict either the instantaneous velocity of the active forelimb and the nose, or the sequence phase, from the spiking activity of groups of simultaneously recorded DLS units. **G**: (Top left) horizontal velocity of the active forelimb from a representative session. Trials are aligned to the first lever press and sorted by trial duration. (Bottom left) Velocity predictions on held-out trials. (Right) Model performance (measured in pseudo-R^2, see Methods), tested on held-out trials. Performance is shown for models trained on every sequence (Full) and tested on a held-out trials, and for models trained on a randomly selected half of the sequences and tested on the other half (Subset). Gray lines indicate model performance within individual rats (n=4). **H.** Heatmaps show observed (top) and predicted (bottom) sequence phase for single sequences without repeated elements (left), and for all flexible sequences (right). Trials are aligned to the first tap. (Right) Model performance, tested on held-out trials and quantified by the pseudo-R^2, for models trained on all flexible sequences (full), and those trained on a single sequence with non-repeating elements (single). *P<0.05, two-sided t-test.

To probe this idea[15], we trained a multilayer neural network to predict, using the spiking activity of simultaneously recorded DLS units, the instantaneous velocity (both horizontal and vertical components) of the rats' active forelimb and nose during the flexible task (Fig. 4f). Consistent with observations from trial-averaged ensemble activity, we could decode movement kinematics on individual trials across the different sequences from populations of DLS neurons (Fig. 4g). Decoders trained on a subset of sequences could predict kinematics from held-out sequences just as well (Fig. 4g), implying that the kinematic code in DLS is invariant to the sequential context of the movements as suggested by our earlier analysis (Fig. 4d-e).

Recent studies[83,91,92], have suggested that DLS encodes the temporal progression of behavior. In the context of stereotyped movement sequences, however, kinematics and time are tightly coupled, making it difficult to parse which of these attributes DLS activity reflects[93–95]. Because our flexible task condition breaks the coupling between time and kinematics, the two become dissociable. Training a decoder to predict the phase of the behavior failed (Fig. 4h), meaning that time in the sequence cannot be recovered from DLS activity alone. Coupling phase and kinematics by considering only single sequences with no repeated motor elements (e.g., lever taps, see Methods for how these were selected), allowed us to decode phase (Fig. 4h). Taken together, our results suggest that DLS encodes low-level continuous kinematics of movements in a way that is - in contrast to prior reports[48,50] – invariant to their sequential context.

The DLS is required for automatic but not cued sequences

Although our neural recordings showed that DLS activity reflects ongoing kinematics in a similar way for flexible and automatic motor sequences, this does not establish a causal role for DLS in their execution. Alternatively, DLS activity could - in one or both modes - simply reflect input from essential sensorimotor control circuits[96]. To arbitrate between these possibilities, we lesioned DLS bilaterally in expert animals (n=5 rats, see Methods, Fig. 5a, Extended Data Fig. 4b).

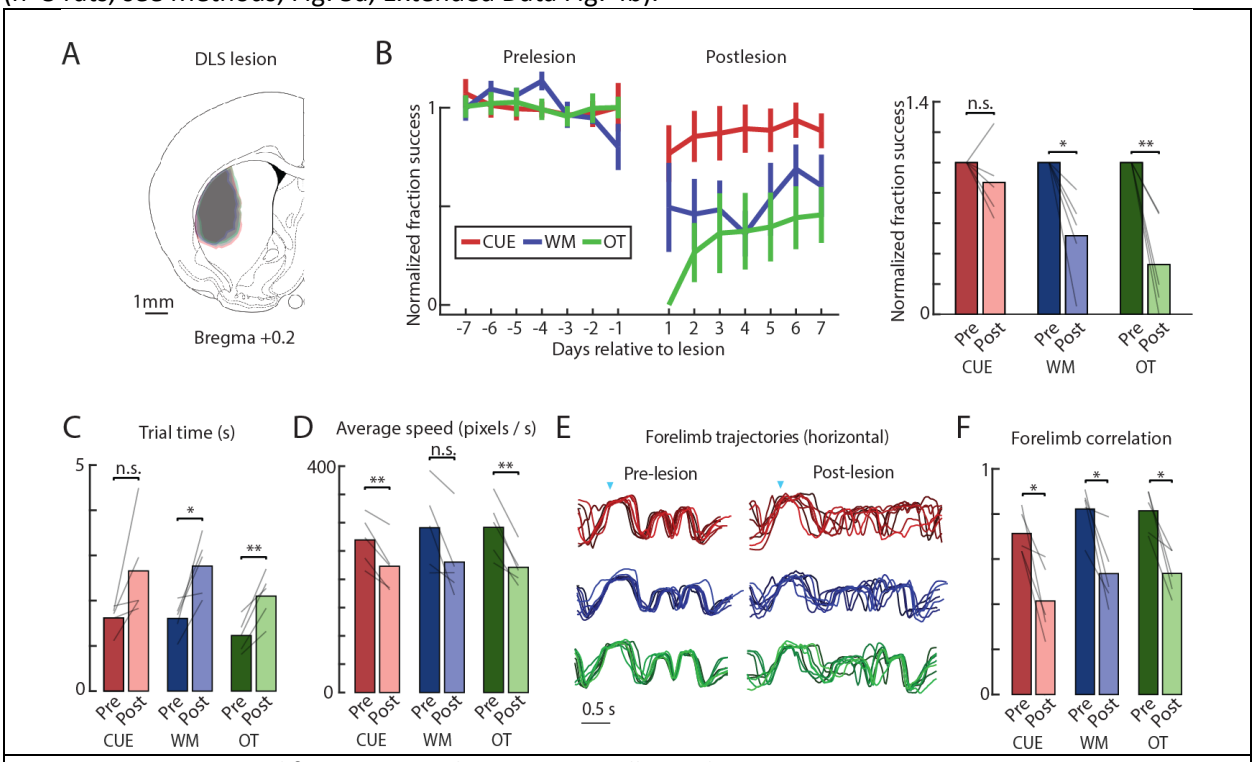

Figure 5: DLS is required for automatic, but not externally cued sequences
A. Outline of DLS lesion boundaries, from 3 rats in one hemisphere. For full lesion annotation, see Extended Data Fig 3. **B.** Left, the success rate, normalized to pre-lesion performance, averaged over rats (n=5, error bars are SEM), in the week before and after lesion. Right, success rate, normalized to pre-lesion performance, in the week before and after lesions averaged across rats. Gray lines denote individual rats. **C-F.** Detailed kinematics and vigor are affected across all three execution modes following bilateral DLS lesion. Trial times (C) and average forelimb speed (D) for the last 1000 trials before, and first 1000 trials after the lesions. **E.** The horizontal position of the active forelimb on eight example trials with similar duration are overlayed and compared (left) and after (right) DLS lesions. **F.** Average trial-to-trial correlation for trajectories of the active forelimb (both horizontal and vertical) before and after lesion. *P<0.05, **P<0.01, 2-tailed t-test.

Following a seven-day post-lesion recovery (see Methods), performance on the OT sequence was severely impaired (Fig. 5b), consistent with a prior report[15]. In stark contrast, performance on CUE sequences was comparable to pre-lesion (Fig 5b). Success rates in WM trials were reduced following the lesion, with the relative drop in performance being less severe than for the OT mode (Fig. 5b). A seven-day control break before the lesion (see Methods), did not significantly affect the behavior in either execution mode (Extended Data Fig. 5).

One possible explanation for the lesion resilience in CUE trials is that visual cues aid movement initiation in a DLS-independent manner[89]. However, the post-lesion drop in performance on OT and WM trials could not be explained by a deficit in movement initiation[55]. Although DLS lesioned rats generated fewer lever-presses overall, they were actively engaged in the task and performed similar numbers of lever-presses across flexible and automatic session types (Extended Data Fig. 6a). DLS lesions also induced a significant increase in variability, or randomness, of the errors across all three execution modes (Extended Data Fig. 6b-c), suggesting that the lesioned rats were more exploratory in their actions.

Taken together, these results are consistent with DLS having an essential role in controlling automatic (OT) and, to a lesser degree, working memory guided motor sequences (WM)[15,44,97]. However, we find that it is dispensable for executing visually guided motor sequences (CUE)[98,99].

Task-specific learned kinematics is affected following DLS lesion.

A unifying explanation for our results is that the BG contribute to learned movement kinematics across both flexible and automatic execution modes[15]. However, automatic sequences become consolidated and specified in terms of low-level kinematics, whereas flexible sequences rely critically on higher-order sequence information, the expression of which may (WM) or may not (CUE) rely on striatum[44,100].

Consistent with a general role for the BG in the specification of learned task-specific movement kinematics [15], we observed similar changes to the orienting and pressing movements after bilateral DLS lesions across the three execution modes. The 'vigor' of the movements, as measured by the trial times and average movement speed, was reduced (i.e. longer trial times and slower speeds, Fig. 5c-d). While this is similar to prior reports on BG's role in controlling movement vigor[42,53], the lesion-induced deficits went beyond affecting overall movement speed and amplitude. Trial-to-trial variability, even for similar duration movements, was also dramatically increased (Fig. 5e-f).

Interestingly, we found that the quality of the movements post-lesion resembled what we see early in learning (Extended Data Fig. 7), a result consistent with DLS specifying learned kinematic modifications to task-related actions and movements[15,17].

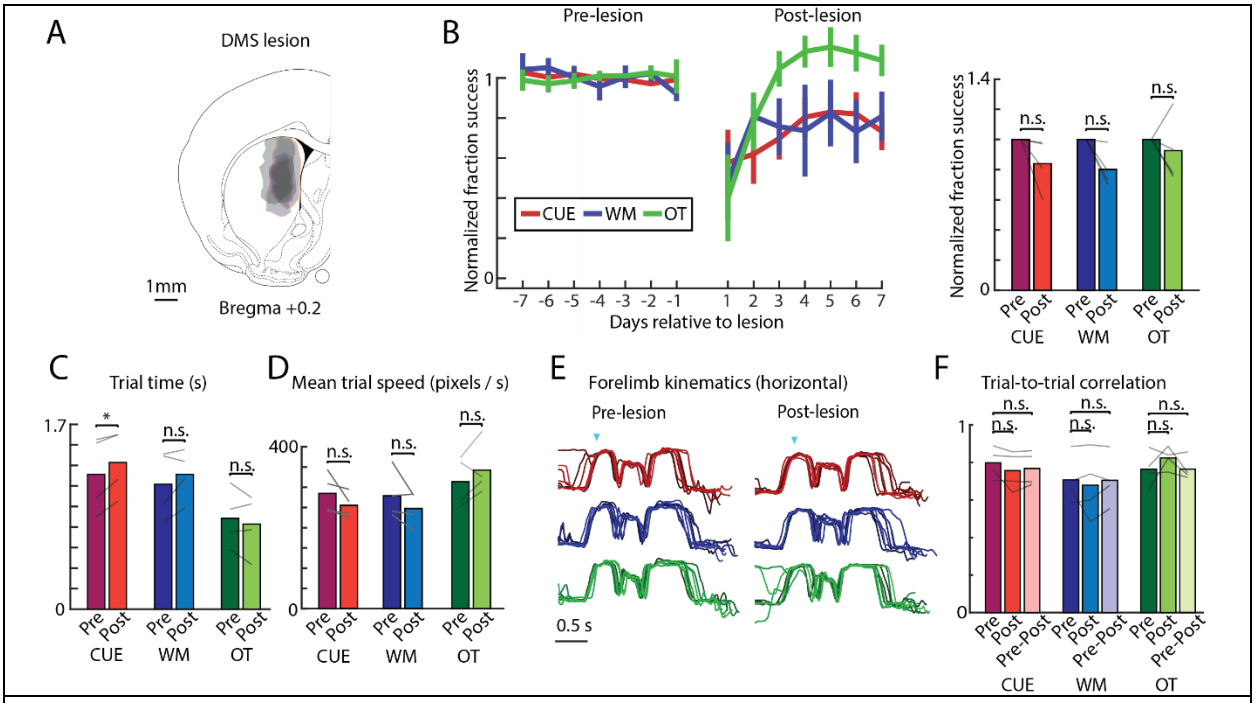

Figure 6: DMS is not required for flexible nor automatic sequence execution

A. Outline of DMS lesion boundaries, from 3 rats in one hemisphere. For full lesion annotation, see Extended Data Fig 3. **B.** Performance in CUE, WM, and OT trials is not significantly affected by bilateral DMS lesions. Left, normalized success rate, averaged over rats (n=4, error bars are SEM), in the week before and after lesion. Right, average normalized success rate across all rats. **C-F.** The detailed kinematics and vigor are not significantly affected b bilateral DMS lesion. **C.** Trial times of the last 1000 trials before, and first 1000 trials after lesion. **D..** Average forelimb speed. **E.** The horizontal position of the active forelimb on 8 example trials with similar durations are shown before (left) and after (right) DMS lesions. **F.** Average trial-to-trial correlation for trajectories of the active forelimb (both horizontal and vertical), before and after lesion, and between pre and post lesions. *P<0.05, paired t-test.

The DMS is not required for flexible or automatic execution

Our focus on sensorimotor striatum (DLS) was motivated by its known role in movement execution[38,54,90]. In contrast to DLS, which receives much of its input from sensorimotor cortex, dorsomedial striatum (DMS) receives its cortical input predominantly from PFC and PPC[101,102]. Though this associative region of the striatum has been implicated in flexible behaviors, such as modifying, switching, and updating behavioral choices in response to previously learned associations[33,58–61], whether it has an essential role in generating flexible motor sequences is less clear[32,76]. Thus, to probe the role of DMS in flexible and automatic motor sequence execution, we lesioned it bilaterally in a separate cohort of expert animals (n=4 rats, see Methods, Fig. 6a, Extended Data Fig. 4c).

Consistent with our previous work[15], DMS was not required for automatic motor sequence execution (Fig. 6b). Interestingly, performance in flexible sessions also remained unchanged following lesions. Unlike for DLS, lesions of DMS did not significantly affect kinematics in either execution mode, with lesioned rats showing no consistent increase in trial time or mean trial speed or a drop in the stereotypy of their task-related movements (Fig. 6c-f). This reinforces the dissociation between the DLS and DMS in terms of low-level kinematic control[15], and further suggests that DMS is dispensable for executing both flexible and automatic motor sequences, at least under the conditions of our task. Whether DMS plays a role in early learning remains an open question[30–32,86,103].

A simple neural network model can account for the results in both CUE and OT execution modes

At first glance, our results showing a nearly identical neural code for kinematics in DLS across execution modes but resilience to DLS lesions only in the CUE mode may seem confusing, as they suggest that the behavior of DLS is both similar (e.g., in terms of coding properties) and different (e.g., for causal manipulations) across modes respectively. To explore this, we built a simple neural network model of the motor system (Fig. 7a). We used this to determine the conditions under which a DLS-like network that learns to interact with 'downstream' control circuits across execution modes gives rise to this seeming discrepancy.

The DLS network in our model contained no recurrence, reflecting the fact that spiny projection neurons are coupled via relatively weak and sparse lateral inhibition[104,105]. The "downstream" component of the model – intended to capture the role of both motor cortex (MC) and brainstem control circuits – was made recurrent. For simplicity, and to focus on the DLS, we abstracted away the details of how it connects to downstream control circuits (i.e., through other BG nuclei, thalamus, etc.), modeling them with a set of linear synaptic weights. To capture the ability of animals to execute cued lever presses prior to sequence training, we pretrained our model to perform a simple in-silico version of 'lever pressing': moving a virtual manipulandum to a target in a 2D environment.

We then trained the DLS input synapses such that our network output moved through sequences of three targets (Fig. 7b). The same network was tasked with producing flexible sequences instructed by external inputs (CUE mode), and also, in the absence of cues, a single internally generated sequence (OT mode; see Methods). As our modeling focused on the differences between flexible and automatic execution modes, we considered only the CUE and OT trial types, setting aside for this analysis the distinction between memory-driven (in WM trials) and sensory (in CUE trials) inputs.

Since animals value time[106] and reduce trial duration as a function of learning (Fig. 1d), our training procedure incentivized the model to reach the three target positions in the correct order as quickly as possible. The decision to train the DLS input synapses was inspired by the presumed role of cortico-striatal and thalamo-striatal plasticity in reinforcement learning[17,60].

To compare the performance of our network model to that of real rats, we conducted analyses of the model analogous to those performed on our experimental data. We found that simulated lesions to the DLS following training impaired OT but not CUE task performance (Fig. 7c; compare with Fig. 5a), recapitulating our experimental results. This is not surprising given the downstream circuit's pretrained ability to generate cue-driven responses. However, several non-trivial experimental results were also captured by our model. First, model DLS lesions affected movement trajectories on CUE trials, decreasing movement velocity and increasing trial time, reflecting a role for DLS in shaping movement kinematics across execution modes following task training (Figs. 7d-e; compare with Figs. 5a-b). Further, the activity of the neural units in the trained DLS network was largely independent of execution mode (Figs. 7f-g; compare with Figs. 3b,d). This cross-mode independence reflects an emergent alignment of DLS inputs (which are trained on both task modes) for OT and CUE trials with the same target sequence (Fig. 7h). Finally, we observed that DLS network representations reflected egocentric direction-of-motion information (Fig. 7i; compare with Figs. 4d-e). Thus, key features of the experimental data – sensitivity of automatic task performance to DLS lesion, invariance of DLS activity to execution mode, and a role for DLS activity in guiding movement kinematics – all emerge naturally during task learning when using a network model with basal ganglia-like circuitry.

In the model, we used a biologically-inspired circuit architecture (Fig. 7a) and matched the training procedure of the network to that of our rats (i.e., with sequence training overlaid on pretrained circuits). To probe how different features of our model contributed to the results, we also considered three alternative circuit models/paradigms. First, to test whether our results depended on DLS output being time-varying and high-dimensional, so as to specify detailed kinematics, we made the DLS output scalar, thus constraining it to represent coarse sequence-level information (e.g. movement speed modulation or 'vigor', as has been suggested[42,53]. This model led to markedly different DLS activity patterns across execution modes, in violation of our experimental findings (Extended Data Fig. 8).

We next explored an 'action selection' model in which DLS is constrained to generate signals only at the boundaries of elementary movements, which inform the rest of the circuit of the next 'lever press' to be executed. This model resulted in DLS activity patterns that lacked prominent representations of egocentric movement information, again in violation of our experimental data (Extended Data Fig. 9).

Finally, to test whether the mode-specific deficits of our lesions were due to the existence of pre-trained motor circuits capable of executing cued movements, we eliminated the pre-training of downstream circuits and trained the full network de novo on all aspects of both task modes (CUE and OT). This simulation failed to capture the DLS lesion resilience seen in our experiments (Extended Data Fig. 10). Comparing the results from our various models with our experimental data lends further support for the idea that, for behaviors with learned task-specific kinematics, the BG provide fine-scale kinematic control signals to downstream circuits, which in the case of automatic motor sequences defines the sequential behaviors.

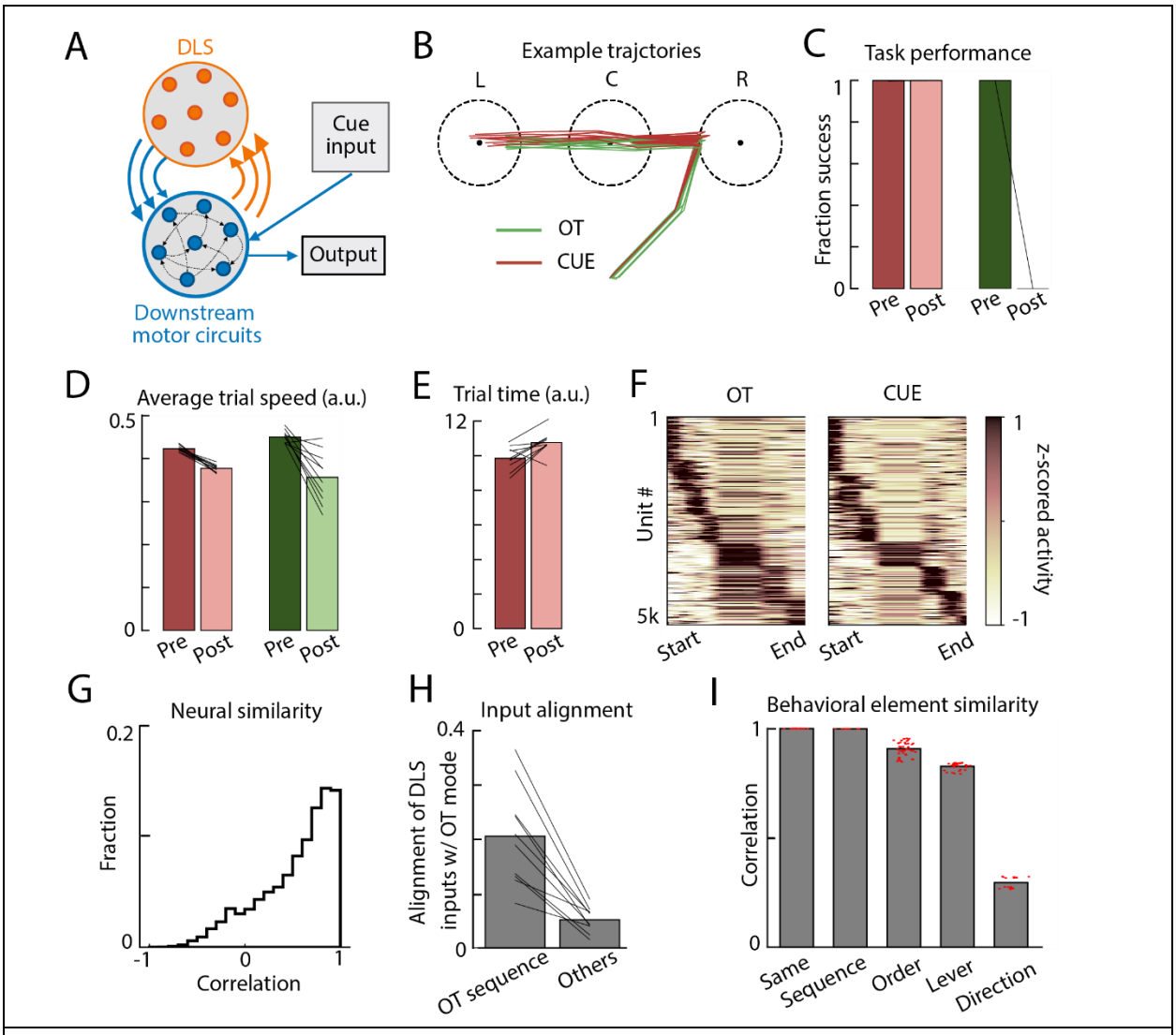

Figure 7: Experimental results emerge naturally during task learning in a neural network model
A. Schematic illustrating architecture of neural network model. DLS weights (orange) are trained on the cued and automatic task modes and interact with downstream recurrent motor circuits already trained to perform cued movements. **B.** Example trajectories on the simulated task. The network controls the velocity of a "forelimb" and must move it into three circular regions (representing "level presses") in the correct sequential order (in this example, RCL for both the CUE and OT modes). **C.** Average trial success rate (defined as successful completion of target sequence). Bars show averages across ten network simulations for each condition, lines depict individual simulations. **D.** Same as C, for trial speed (average magnitude of velocity, in arbitrary simulation units). **E.** Same as C and D, for trial time (i.e., number of simulation time steps). **F.** Average Z-scored activity of model neurons in the DLS population during execution of successful OT and cued trials with the same target sequence. Neurons are displayed in the same order in both plots. **G.** Histogram over all model DLS neurons of correlation across task modes of trial-averaged activity, as in Fig. 3d. **H** Correlation between input to DLS units across modes. Line segments indicate individual simulations; bars indicate averages cross simulations. Left: correlation between DLS inputs on OT and cued trials for the same sequence. Right: same measurement but shown for cued trials with other target sequences (averaged over all other sequences). **I.** Correlation in model DLS population activity between pairs of sequences, as in Fig. 4d.

Discussion

To probe the neural circuit implementation of 'automatic' and 'flexible' motor sequences, we developed a 'piano-task' in which rats generate three-element lever-press sequences in two basic conditions: (i) when the rewarded sequence is predictable and overtrained ('automatic' sessions) and (ii) when it is unpredictable and instructed by cues ('flexible' sessions) (Figs. 1,2). In contrast to similar studies in humans and NHPs, which focused primarily on primate-specific cortical brain regions[6,22,43,77,78,107], we probed the role of the striatum, a highly conserved part of the mammalian motor system[108] widely implicated in action selection and movement control[38,90]. Neural activity patterns recorded in its sensorimotor arm were similar when the same motor sequence was generated in the automatic vs the flexible mode (Fig. 3), representing low-level kinematic features of the movements (Fig. 4). While lesions of the DLS affected task-specific movement kinematics across all execution models, higher-level sequential organization of the behavior remained unaffected for visually cued flexible sequences but not for automatic ones (Fig. 5). DMS lesions had no effect on either performance or movement kinematics (Fig. 6). A simple network model could recapitulate these results and suggests a mechanism: DLS learns to transform its inputs in both flexible and automatic modes into mode-invariant activity patterns that provide similar kinematic control signals to downstream motor circuits (Fig. 7).

No neural signatures of 'chunking' or action selection in the DLS

While flexible motor sequences are assembled on-the-fly in response to unpredictable environmental cues and conditions, automatic behaviors are internally generated and expressed the same way every time. Behavioral and neurophysiological studies have suggested that such overtrained motor sequences become 'chunked' (e.g.[8,49,109]), meaning that sequences of motor elements, initially generated by a serial decision-making process, become linked in way that allows the sequence to be selected and executed as a single action[110,111]. This has the potential benefit of reducing the computational cost associated with often-used motor sequences and making their execution more robust to cognitive interference[2,10].

The BG have been widely implicated in the process of chunking[110], with studies showing the neural representation of task-specific motor sequences in BG becoming sparser with extended practice [46,50,112], with peaks in population activity marking the boundaries (i.e. start and stop) of overtrained 'chunked' behaviors[46,48,50]. Such a sparsification is consistent with a role for the BG in selecting actions elaborated in downstream circuits[46,112,113]. For flexible behaviors, action selection would occur at the level of individual elements and hence be more granular, while selection for overtrained behaviors would happen at the level of the whole sequence or 'chunk'.

Though a compelling interpretation of some neurophysiological findings[51], an increasing number of studies have failed to see start/stop activity even in highly overtrained and stereotyped motor sequences[15,56,90,103]. Our paradigm allowed us to directly probe whether DLS activity reflects the delineation and selection of motor chunks by comparing it for the same sequence in an automatic (selection of the sequence as a chunk) versus flexible (serial decision making and selection) context. Not only did we not see prominent start/stop activity in the automatic context, but we also found that flexible and automatic motor sequences share highly correlated representations in the DLS (Fig. 3).

How should the differences between our results and those showing signatures of chunking and - implicitly - the selection of overtrained sequences by the BG be interpreted? First, most studies implicating BG in these processes tend to compare overall activity early in learning to what is seen in the expert (see, e.g. [21,30,49,86,112]). Any observed activity difference could thus reflect either the development of chunking or of learning-related changes in movement kinematics. Here we instead compared automatic, or 'chunked', behaviors to highly trained but flexible behaviors with similar kinematics. That we see no difference across the conditions suggests that start/stop activity seen in previous studies may not be a consequence of motor chunking per se but may instead reflect learning-related changes in motor output or a shift in how the DLS contributes to it.

In many cases, studies reporting start/stop activity in the BG[47,48,50,103] do so in the context of overtrained behaviors that have become habitual, i.e., reflexively expressed irrespective of their predicted outcome[62,84,114–116]. This has the potential to confounds two independent processes, the development of motor automaticity and habit. Indeed, many of our 'automatic' actions, such as signing your name or serving in tennis, are not habitual[117], and conversely, many of our habitual behavioral programs can be quite flexible[118,119]. The lack of prominent start-stop activity in our task, seen in other paradigm on overtrained habitual behaviors, is thus consistent with it being a signature of habit formation and not motor automaticity, though we must also note that there are studies of overtrained habitual behaviors with no prominent start/stop activity in the BG[83].

Alternatively, the lack of start/stop activity in our study could mean that the motor sequence we overtrained failed to coalesce into a single 'chunk' due to some peculiarity of our experimental approach. We do not find this plausible, given the clear signatures of automaticity we see (Fig. 2a-d) and the lengthy training times. Furthermore, in an earlier study, in which we trained rats to generate highly stereotyped and stable movement patterns without any need for flexibility, we similarly did not see start/stop activity[15].

But irrespective of whether the full automatic motor sequence was 'chunked', the orienting and forelimb movements for pressing the lever – repeated hundreds of thousands of times during training in our task – are behavioral elements that can be selected for execution and sequentially ordered. Prior studies, including on natural behaviors[87,120], have suggested that the BG contribute to the selection and ordering of such motor elements[29,87]. The proposed scheme is similar to what we discussed above for chunked sequences: neural populations tuned to specific elements or 'chunks' increase their activity at the transition to that element, with the presumed effect of activating downstream circuits generating it [87,110]. In our recordings, however, we did not find the transition times between discrete elements to be privileged in terms of population activity. The continuous activity we observe, combined with our failure to observe higher-level features of the motor sequences, such as the ordinal position of motor elements or their sequential context (Fig. 4d), suggest that the BG may not be essential parts of the serial selection process that underlie flexible motor sequences. This was corroborated experimentally: neither DLS nor DMS lesions affected serial selection performance in our visually-guided flexible sequence task (Figs. 5b & 6b). This was further supported by our network simulations: when we constrained DLS to operate as an action selector, our model's performance and the activity of its units no longer recapitulated our experimental observations (Extended Data Fig. 7b).

While our results do not support a role for the BG in initiating consolidated motor chunks elaborated downstream, they are consistent with overtrained behavior becoming defined as BG-dependent motor chunks. Thus, rather than selecting them, BG's role in motor chunking could be in transforming discrete motor sequence into single continuous actions in which the sequential structure of the overtrained behavior is fully specified by BG-dependent low-level kinematics.

Our results are consistent with BG specifying learned kinematics

While a growing number of studies have suggested that DLS may indeed specify the detailed kinematics of learned movement patterns[15,55,56,83,90], dissociating such a function from a putative role in controlling the temporal progression of overtrained behaviors has been difficult. This is due to kinematics and time being intrinsically linked in stereotyped behaviors[83,94,95]. Our flexible motor sequence task breaks this link, allowing us to dissociate the two coding schemes. In doing so, we found that a decoder could predict the full movement trajectories on a sequence even if it had never been trained on it (Fig. 4h). A decoder trained to predict sequence phase, however, failed (Fig. 4h).

Consistent with a role for the DLS in specifying low-level time-varying kinematics, lesions affected task-specific movements across execution modes (Fig. 5e-f). Lesioned animals could orient towards levers and press them and, in the 'flexible' mode, do so in the correct sequence, but the speed and variability of their movements reverted to what we observed early in learning (Extended Data Fig. 6a-e). This is consistent with a role for the BG in the task-specific refinement of species-typical movements that are generated in downstream circuits, likely in the mid/brain brainstem. We saw a similar result in our circuit model: when a 'DLS' circuit was allowed to interact with pre-trained 'downstream circuits' that could independently respond to cues, variability in trial duration decreased following sequence learning and increased following DLS lesion for both automatic and flexible execution modes (Fig. 7d-e). Dissecting the model revealed that, despite receiving different inputs across modes, the DLS learned mode-invariant activity that modulated movement kinematics through its downstream targets.

Whereas the detailed kinematics of the learned behaviors were affected, the sequential organization of visually guided motor sequences survived DLS lesions. That the same sequence was impaired in automatic sessions is consistent with overtrained sequential behaviors (motor 'chunks') becoming defined in terms of their low-level kinematics, a specification that depends critically on the BG[15].

Distinction between WM and visually guided.

Prior studies have contrasted the BG's role in memory-guided and visually-guided motor sequence generation[43], showing that the BG are more active[45,100] and its neurons more modulated[41,121] during the execution of memory-guided sequences. There are also reports of working memory-related activity in the striatum, and effects on working memory-guided performance after DMS inactivation[122,123]. Studies in de novo Parkinson's patients, showing that they perform worse in a working memory task than healthy controls independent of the severity of their motor symptoms, further point to a role for the striatum in working memory-guided behaviors[97,124].

This distinction between the BG's contributions to visually and working memory-guided motor sequences were mirrored also in our results (Fig. 5). Though the neural activity patterns in the two conditions were highly correlated (Fig. 3), our study was not designed to assess the time period leading up to the task-specific behavior, leaving open the possibility that there may be signatures of working memory processing in the preparatory phase, as has been observed in DMS in a different task paradigm[122]. Interestingly, lesions of DMS, a region implicated in working memory in other studies[123], did not cause performance deficits in our paradigm. Instead, it was DLS lesions that degraded performance in WM trials, suggesting that activity in the sensorimotor arm of the BG may be necessary for working memory in our task.

While DLS is essential for internally generated motor sequences, both flexible and automatic, visually guided sequences can be generated, albeit with somewhat altered kinematics, without it. This, again, mirrors what is seen in Parkinson's patients, whose struggles to execute internally generated movements can be rescued by providing instructive visual cues[24,125]. The specific role(s) of the BG in different types of internally generated behaviors remains poorly understood. Our paradigm, however, provides a tractable experimental paradigm to parse this in future studies.

What controls flexible behaviors?

Our result suggesting that visually-guided flexible motor sequences can be BG independent raise questions about the identity of the circuits that control this class of behaviors. Work in humans and NHPs have suggested a role for cortex[19,78,126,127]. Though we have shown that motor cortex is not required for executing highly overtrained automatic behaviors in rodents[16] and further developed a mechanistic model explaining how behaviors that are cortically dependent during learning can become subcortically consolidated[128], it remains an open question whether and how motor cortex contributes to flexible motor sequencing and the degree to which its function differs across task modes. Work on skilled reaching

movements instructed by visual input has implicated motor cortex in their execution[129], suggesting that the need to respond to environmental cues may render motor cortex a necessary controller. Future experiments will be needed to address the degree to which motor cortex's contributions to movement control depend on the specific challenges posed by a task, and the condition under which its function require the BG.

Modeling suggests BG representations and function emerge through learning to meet task demands
A model simulating the role of DLS within a larger control network could account for our experimental results, providing a compact description of DLS function in learned motor sequence execution. In our model DLS's role was a direct function of the pre-existing capabilities of other motor circuits and functioned to augment those according to the demands of the task. Specifically, the presence of extra-BG circuits capable of executing cued lever-presses left DLS to refine movement kinematics in the flexible mode and obligated it to learn the entire sequence in the automatic mode. A direct prediction of our model is that performance will not be resilient to DLS lesions when animals are trained to perform sequence tasks for which the *elements of the sequence* are not in the animals' repertoire prior to training. Our model also suggests that DLS can learn to control highly stereotyped behaviors (e.g., ones like our automatic task for which future actions are perfectly specified by past actions) without requiring sensory inputs. In this case, it should be possible to lesion motor regions not instructive to the behaviorally relevant dynamics without impacting task performance (e.g., as seen with motor cortical lesions[15,16]). Conversely, tasks which require substantial unpredictable external guidance (e.g., our flexible task) should be hard or impossible to consolidate into sub cortical loops involving DLS and would remain susceptible to such lesions.

In summary, our results clarify the role of striatum in learned motor sequence execution, showing that its sensorimotor region helps specify task-specific kinematics. For stereotyped automatic motor sequences, our results suggest that the discrete elements of the sequence become linked into a single sequential action specified in terms of BG-dependent low-level kinematics. Importantly, for flexible motor sequences instructed by external cues, the underlying serial decision making process is not contingent on either sensorimotor or associative striatum, suggesting that this process is elaborated in circuits outside the BG.

Methods:
Animals:
The care and experimental manipulation of all animals were reviewed and approved by the Harvard Institutional Animal Care and Use Committee. Experimental subjects were female Long Evans rats 3- to 8-months at the start of training (Charles River).
Behavioral apparatus:
Animals (n=18 total) were trained on our discrete sequence production task (the 'piano' task) in a fully automated home-cage training system[130]. Hardware was controlled by Teensy 3.6 and experiments and videos were recorded by Raspberry Pi 3. Home cage training was done in custom-made behavioral boxes. Boxes were outfitted with three levers spaced approximately 2.5 cm apart, and 14 cm above the floor. Plastic slits 0.64cm thick were placed between each lever to ensure rats press the levers with their forelimbs and not their snout. A reward spout for water delivery was placed beneath the center lever. Lever presses were registered when lever displacement reached a threshold, corresponding to an angular deviation from horizontal of ~14 degrees. Lever displacements were measured by optical sensors (Digi-key QRE1113-ND).

Behavioral training:

Water deprived rats received four 40-minute training sessions during their subjective night, spaced 2 hours apart. Starts of sessions were indicated by blinking house lights, a continuous 1kHz pure tone, and a few drops of water. At the end of each night, water was dispensed freely up to the daily minimum (5ml per 100g body weight).

Stages of training

1. Rats were initially pre-trained to associate a visual cue with a lever press. On each trial, one of three LEDs above each of the three levers, chosen randomly, would light up to signify the 'correct' lever. Correct presses were rewarded while incorrect presses triggered a 1.2 second timeout, which was retriggered for every press in the time out period. To prevent rats from only selecting a single lever, we gradually decreased the probability of cueing a repeatedly pressed lever. All rats (n=18) learned to associate levers with cues in a median of 5284 trials. The criterion for learning was performing at >90% success rate for >100 trials.
2. After learning to associate visual cues with levers, rats were rewarded only when performing consecutive lever presses. Initially rewards were provided for every two successful consecutive presses, but after 500 rewards, reward was dispensed only after every three consecutive lever presses. Cued levers were constrained to not repeat, giving 12 different possible three-lever sequences. Rats quickly learned to press levers in a sequence, and no longer visited the reward port in between consecutive presses.
3. Following 1000 successful three-lever trials, rats were introduced to the block structure (Fig. 1a), which was modeled on a sequence task in primates[79]. In the block structure, the same three-lever sequence is cued on each trial until there are 6 successful performances, then a new sequence is randomly chosen.
4. After ~1-2 weeks of training on the block structure, working memory (WM) trials were introduced by withholding the 2nd and 3rd cued lever in the 4th-6th trial of the block. Missed uncued levers were not required to be repeated until successful for a new sequence to be chosen.
5. One of the four nightly flexible sessions was changed to an automatic session. In this session, rats were required to perform only a single three-lever sequence, chosen randomly for each rat. This sequence was initially fully cued. Cues were then removed in reverse sequence, from last lever to first lever, every time the rat performed at >50% success rate over 30 trials. If success rate fell below 20% for 30 trials, or if rats failed to press the lever once in the entire session, a cue would be added back in. All rats were able to perform > 100 trials with at least two of the three cues withheld after 1024 ± 438 (mean ± SEM) trials or 17 ± 10 (mean ± SEM) days. After learning the sequence without cues, they would occasionally (5.18% ± 1.39% (SEM) of trials) hit the lower threshold prompting the addition of cues.

Behavior analysis

In total, 18 rats were trained on the three-lever task. 12 of 18 were used to characterize the behavior; six were excluded because kinematics was not captured or analyzed early in training.

Definition of expert performance

Expert performance was determined when success rates and trial times stabilized to within 0.5σ of final performance values (based on the last 2000 trials). Metrics (success rates and trial time) were smoothed with a moving average of 400 trials. Furthermore, we required automatic performance to reach >72% success rates to be considered 'expert', following previous studies[49,83,86,129].

Calculation of performance metrics

<u>Success rate:</u> Success rate was defined as the number of rewarded trials divided by the total number of attempted trials.

Trial time: Defined as the interval between the first and third lever press. This only includes successful sequences, as incorrect sequences may not include three full lever presses.
Error variability: Defined as the Shannon entropy (in bits) of the probability of each sequence occurring for a given target sequence. Low probability sequences ($p<0.001$) are discarded. If mistakes are systematic, the probability distributions will be skewed towards particular erroneous sequences, and the entropy will be low. If mistakes are made randomly, the distribution will look more uniform, and the entropy will be high. For flexible sequences, the error calculation was done on the sequence chosen for the OT mode.
Error modes: Motor errors were defined as failures to touch or fully depress the 'correct' lever in what would otherwise have been a correct sequence (Supplementary Movie 2). I.e. the rat oriented to the 'correct' lever and swiped at it but failed to depress it beyond the threshold for detection. Sequence errors, on the other hand, involved orienting to and pressing the wrong lever. For each rat and session type (flexible and automatic), ~100 videos of error trials were manually inspected and labeled as either a sequence or motor error. To analyze behavior following different error mode types (Fig. 2f), we used a heuristic to automatically estimate and classify failures as motor or sequence errors (Extended Data Fig. 3). This allowed us to analyze >100 trials. In this analysis, motor errors were classified as any error sequence that resembled an omitted lever (e.g., for the target sequence LRC, RC and LC are considered motor errors), while sequence errors are any other type of mistake (Extended Data Fig. 2a). This heuristic generally overestimates motor errors (29.65% ± 5.9% of errors for CUE trials, 16.95% ± 5.48% of errors for WM trials, 13.16% ± 5.32% of errors for OT trials, data is mean ± s.e.m.) and underestimates sequence error (Extended Data Fig. 2b). Trial-dependent accuracies and trial times, conditioned on the type of trial that came before (hit, motor error, sequence error), were then calculated using this heuristic (Fig. 2f). For trial times, we only considered sequences that had the same overall movement length as the overtrained sequence (since L→R is further to travel than L→C) as a control.
Average forelimb speed: Raw trajectories (position traces) of the active forelimb were smoothed and up-sampled (from 40hz to 120hz) using cubic smoothing spline (csaps in Matlab, smoothing parameter of 0.1). Instantaneous velocities for the horizontal and vertical positions were calculated, then converted to instantaneous speed. This value was averaged from 0.1 second before the first lever press to 0.1 second after the last one. Since velocity was calculated from a side-view camera, and animals moved towards and away from the camera to press different levers, we couldn't calibrate pixels/s to cm/s, which would require depth information not available to us.
Smoothness metrics: To quantify the smoothness of the movement, or its continuity and non-intermittency[131], we applied three dimensionless quantitative metrics: the negative log-dimensionless jerk, the spectral arc length, and the speed metric[132–134]. These metrics cover three different classes of smoothness parameters: velocity, acceleration, and arc-length based metrics[133]. Values closer to 0 are defined as more smooth.

Trial selection for behavioral analysis
In figure 1, early performance is taken from the first 1000 trials, and late performance is measured from the last 1000 trials. For figure 2, metrics are calculated from all trials after expert performance was reached. For figure 5 and 6, pre- and post- lesion accuracies are calculated from the week before and after lesion. Pre- and post- lesion trial times, trial speeds, and kinematics are taken from the last 1000 trials before and after lesion. Finally, it is important to note that since automatic sessions are introduced after the flexible sessions, early performance on automatic (OT) trials benefits from prior flexible practice (Fig. 1, Extended Data Fig. 7).

Kinematic tracking

To track the movements of the rat's active forelimb and head during our task, we utilized recent machine learning approaches to detect keypoints from individual video frames. Videos of animals performing the task were acquired at 40 Hz (90 Hz for DLS recording cohort) from cameras pointing at the lever from the two sides to obtain both forelimb trajectories, and one camera pointing down from the top to obtain the rat's horizontal position. For video-based tracking, we trained ResNet-50 networks pretrained on ImageNet, using DeeperCut (https://github.com/eldar/pose-tensorflow)[80]. To refine the tracking for our rats, we randomly selected about ~200 frames per view and trained the network using manually labeled position of the hand and nose. The network was then used to predict the position of body parts across all trials on a frame-by-frame basis, using GPUs in Harvard Research Computing cluster. Tracking accuracy was qualitatively validated post-hoc by visual inspection of 5 trials across 3 different sessions. Frames with poor tracking (< 0.95 score from the model), due to occlusion of the forelimbs, were removed and trajectories in those frames were linearly interpolated. If > 5 consecutive frames were removed, the trial was discarded for tracking purposes. Additionally, any trial with >5% of poorly tracked frames was removed from the analysis. The full trial trajectory was then smoothed using a Gaussian filter in matlab, with a σ of 0.6 frames.

Kinematic analyses

To quantitatively compare kinematic similarity, we computed pairwise trial-to-trial correlations. Since trial times varied, movement trajectories were time warped to a common template. Specifically, trajectories from each trial were interpolated so that the time between the 1st and 2nd lever, and the time between the 2nd and 3rd lever, matched the median inter-lever intervals. Though we tracked both forelimbs, analyses were performed only on the active forelimb used to press the lever. Rats used a single forelimb to perform lever presses (n=11/18 right, n=7/18 left).

Electrophysiological recordings

Microdrive construction, surgical and recording procedures were performed as previously described[135]. After expert performance was reached on the flexible and automatic tasks, a microdrive containing arrays of 16 tetrodes was implanted into the DLS (n=4 rats) contralaterally to the active forelimbs as previously described[15] (Extended Data Fig. 4a). Neural and behavioral data was recorded continuously for 95+-31 days. The drive was occasionally advanced by ~200 µm, 0-4 times over the course of the experiment. At the end of the experiment, an electroylytic lesion was done to mark the electrode site. This was done by passing a 30 µA anodal current for 15s through the electrode tips. For implant coordinates, according to Paxinos[136], see Table 1.

Lesion surgeries

After reaching expert performance, bilateral striatal lesions were performed (n=5 DLS, n=4 DMS) as previously described[15]. For injection coordinates, see Supplementary Table 1. In brief, quinolinic acid (0.09 M in PBS (pH 7.3), Sigma-Aldrich) was injected in 4.5nl increments, via a thin glass pipette connected to a microinjector (Nanoject III, Drummond). Lesions were performed in two stages, starting with the side contralateral to the primary forelimb (the forelimb that presses the first lever). Animals recovered for 7 days before being reintroduced to training.

Table 1: Surgical coordinates and injection volumes

	DLS lesion				DLS implant	DMS lesion			
AP	+0.7	+0.7	-0.3	-0.3	0.5	+1.2	+1.2	+0.2	+0.2
ML	±3.9	±3.9	±4.1	±4.1	±4.0	+2.2	+2.2	+2.0	+2.0

DV	-4.5	-3.5	-4.8	-4.0	4.0	-4.4	-3.4	-4.4	-3.4
µL	25*4.5	19*4.5	20*4.5	16*4.5		25*4.5	25*4.5	25*4.5	25*4.5

Histology

At the end of the experiment, animals were euthanized (100 mg/kg ketamine and 10 mg/kg xylazine), transcardially perfused with either 4% paraformaldehyde (for nissl staining to confirm lesion size and location), or 2% paraformaldehyde (PFA) and 2.5% glutaraldehyde (GA) (for osmium staining, to confirm location of electrode implant) in 1x PBS. For electrode implants, brains were then stained with osmium (as described in[137]) and embedded in epoxy resin for micro-CT scanning. Micro-CT scans (X-Tek HMS ST 225, Nikon Metrology Ltd.) were taken at 130 kV, 135 uA with 0.1 mm copper filter and a molybdenum source. 3D volume stacks were reconstructed (VG studio max), and brains were aligned along the coronal, medial, and sagittal plane using Fiji. Location of the electrolytic lesion could be calculated relative to anatomical landmarks (i.e., corpus callosum split at AP = 1.65mm from bregma, anterior commissure split at 0 mm bregma). For lesioned animals, brains were sectioned into 80-µm slices using a Vibratome (Leica), then mounted and stained with Cresyl-Violet. Images of whole brain slices were acquired at x10 magnification with either a either a VS210 whole slide scanner (Olympus) or an Axioscan slide scanner (Zeiss). To quantify the extent and location of striatal lesions, we analyzed coronal sections spanning the anterior posterior extent of the striatum from 4 calibration animals (DLS) (7 hemispheres injected in total) or from 4 experimental animals (DMS). Boundaries were manually marked based on differences in cell morphology and density[138,139]. The extent of the striatum was determined based on the Paxinos[136], using anatomical landmarks (external capsule, ventricle) and cell morphology and density.

Neural analysis

Spike sorting

Raw neural data was collected continuously over the course of the experiment (mean and s.e.m. are 95 ± 31 days, n=4 fully trained rats). Spiking activity from populations of single units was sorted using our custom-designed spike-sorting algorithm, Fast Automated Spike Tracker (FAST)[135]. A custom Matlab GUI (https://github.com/Olveczky-Lab/FAST-ChainViewer) was used to manually isolate and track single-units over long timescales. On average, we isolated 20.5 ± 13.3 units simultaneously in the striatum within each session. We were able to track units for an average of 4.3 ± 1.2 days. Assessing the quality of sorted single unit was done as previously described[135]. In brief, we evaluated unit quality by computing the isolation distance[140], the L-ratio[141], the fraction of inter-spike interval violations[142,143], discarding units that did not meet our criteria (Isolation distance >=25, L-ratio <=0.3, and ISI violations below 2m <= 1%).

Criteria for unit selection

We selected a subset of the total population of recorded units for our neural analyses. To be included, we required that a neuron fired at least 1 spike, on at least 25% of all trials and was recorded over >5 rewarded trials in each execution mode (CUE, WM, OT) for figure 3, or >5 rewarded trials in each of the 12 different sequences. From a total of 2468 recorded and well-isolated units, this criterion reduced the units available for analysis to 579 units for the comparison across execution modes, and to 340 units for comparisons across sequences in the flexible sessions.

Neural metrics

Trial averaged, z-scored activity: First, instantaneous firing rates were calculated for each trial by convolving binned (10ms bins) spike counts with a Gaussian kernel (σ=25ms). To account for differences in trial times, firing rates were then local linearly warped to the median press times. Warping was done only after calculating firing rates so as to not artificially increase or decrease the firing rate. Firing rates before the first and after the last lever press were not warped. After this alignment step, each trial was z-scored, and then averaged over for each unit and each execution mode.

Average firing rates: Firing rates on individual trials were calculated from -0.2 seconds before the first lever press, to 0.2 seconds after the third lever press. This value was averaged over every trial for a given execution mode.

Average activity: To determine if there was elevated population activity at privileged timepoints in the sequence in the task (e.g. at the boundaries of discrete motor elements), we averaged over the time varying z-scored activity for each unit recorded in a rat. This average trace was compared to a distribution of average z-scored activity, sampled from random times in the behavior (2 seconds before and after the first and last lever press, n=1 x 10^4 permutations).

Correlation across execution modes: For each unit, correlation coefficients were computed between the time-varying vector of trial-averaged activity across execution modes.

Correlating neural activity associated with behavioral elements across sequences:
We computed the correlations between neural population vectors of combined orienting and lever pressing movements across the 12 different sequences. Population vectors were calculated by averaging the activity of each neuron over orienting and lever press movements. Orienting movements were defined as those that occurred 0.1 seconds after a prior lever press until 0.1 seconds before the next press. Lever press movements were defined as occurring +/-0.1 seconds around the lever deflection. We excluded the first lever press for this analysis, as it was not preceded by an orienting movement.

Principal components: Principal component analysis was performed on the matrices of population activity (neurons vs. time) concatenated across either the three execution modes (CUE, WM, OT) or the twelve sequences along the time dimension. Execution modes or sequences were then disjoined to generate the plots in Fig. 3e and Fig. 4d.

Neural decoding analysis
We used a feedforward neural network with two hidden layers to predict the time-varying vertical and horizontal velocity components of the active forelimb and the nose from the spiking activity of ensembles of DLS neurons. Spiking activity was binned in 25ms bins. We used 75ms of coincident spiking activity as the input to the model. Other model parameters were the same as in previous work[15].

We trained our models on blocks of >50 trials in which there were at least 12 simultaneously recorded units that had an average firing rate >0.25hz during the trials. In each block of trials, we fit decoding models using the activity of up to n=20 randomly sampled ensembles of 12 striatal units. We quantified model performance on a balanced test dataset by computing the pseudo-R2: $pR^2 = 1 - \frac{\Sigma(X-\hat{X})^2}{\Sigma(X-\underline{X})^2}$
Decoding performance (pseudo-R2) was measured in each ensemble, then averaged across all 20 ensembles, and then averaged across all blocks of trials for each rat. For subset model, the training dataset was generated from only 6 of the 12 sequences, chosen at random for each of the n=20 ensembles. The test dataset was then generated from the remaining 6 sequences.

Neural network model

We simulated an artificial neural network consisting of two populations, one corresponding to DLS and another to other downstream motor circuits. The DLS network contained no recurrent connections while the downstream network contained all-to-all recurrent weights. The two populations were bidirectionally connected with all-to-all feedforward and feedback weights. The downstream motor network directly controls movement via a set of feedforward weights, and also receives an additional source of input representing cue signals via a set of feedforward weights. Each network consists of 500 units with a rectified linear (ReLU) activation function. Network weights were initialized with the Kaiming Uniform initialization[144]. Gaussian noise of standard deviation 0.1 was added to the inputs to each neuron in both networks at every timestep in all simulations.

We modeled a simplified version of the experimental task in which the output of the network controls the velocity of a "forelimb" (represented simply as a point) and is tasked with moving it into a set of three circular target zones in a prescribed sequential order, as in the piano task. The target zones were positioned as shown in Fig. 7b. On each trial, the loss function measuring the performance of the network was defined as the sum of the squared distance between the forelimb position and the center of the current target. The identity of the current target changes to the next in the sequence once it is reached. On cued trials the target lever changed, and on the first step, cue input was provided in the to the downstream network in the form of a vector indicating the position of the cue relative to the forelimb. The cue input was transient, lasting only one timestep for each cue. If the sequence was not performed successfully within T=40 timesteps of the simulation, the trial was halted and considered a failure.

The network, excluding the DLS input and output weights, was pre-trained on the cued task for 100,000 iterations (well past the point where asymptotic performance was reached). The DLS input weights were then trained on randomly interleaved cued and automatic task trials (50% probability of each, with all 12 possible target trajectories equally likely on cued trials), again for 100,000 iterations. The target sequence on automatic trials was always the same (right, center, left). All network training used backpropagation and the Adam optimizer with learning rate set to 1e-4. Training was conducted using PyTorch.

In Extended Data Fig. 8, we modified the network architecture by replacing the NxN DLS output weights with a chain of Nx1 and 1xN weights, corresponding to a rank-1 projection. In Extended Data Fig. 9, we modulated the gain of DLS activity, suppressing it by a factor of 0.1 at all time steps except the first and those when the target lever changed. In Extended Data Fig. 10, we omitted the pretraining stage and instead trained the entire model on all task modes for 200,000 iterations.

Extended Data:

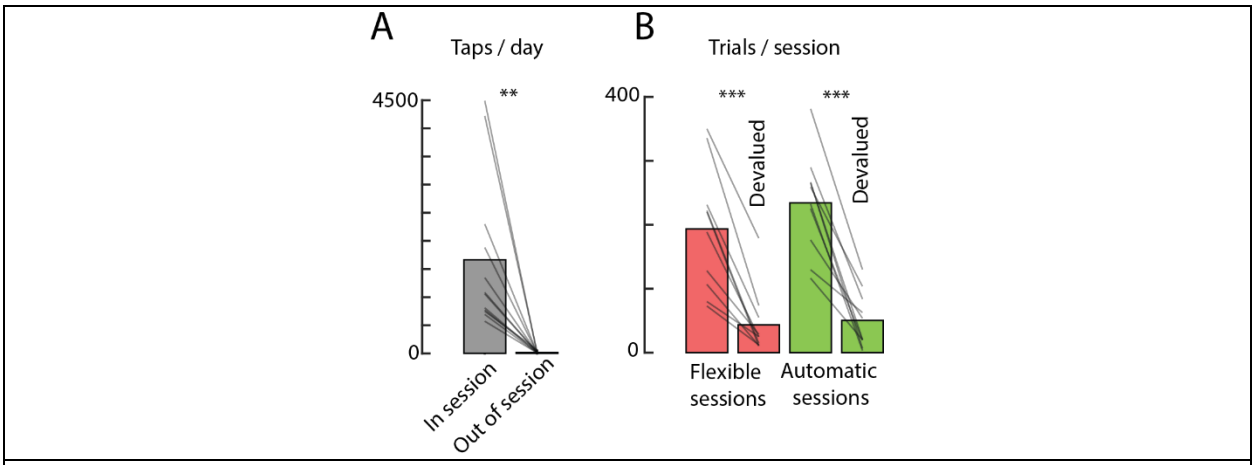

Extended Data Figure 1: Rats express flexible and automatic behaviors in a goal directed way
Left, average number of taps performed per day. Homecage trained rats engage with the levers, which are always present, only during session times. Right, average number of trials per session, plotted for flexible (red) and automatic (green) sessions, for typical and devalued sessions (see methods). Bars indicate the grand average across rats, and lines are individual rats. **P<0.01, ***P<0.001, two-sided t-test.

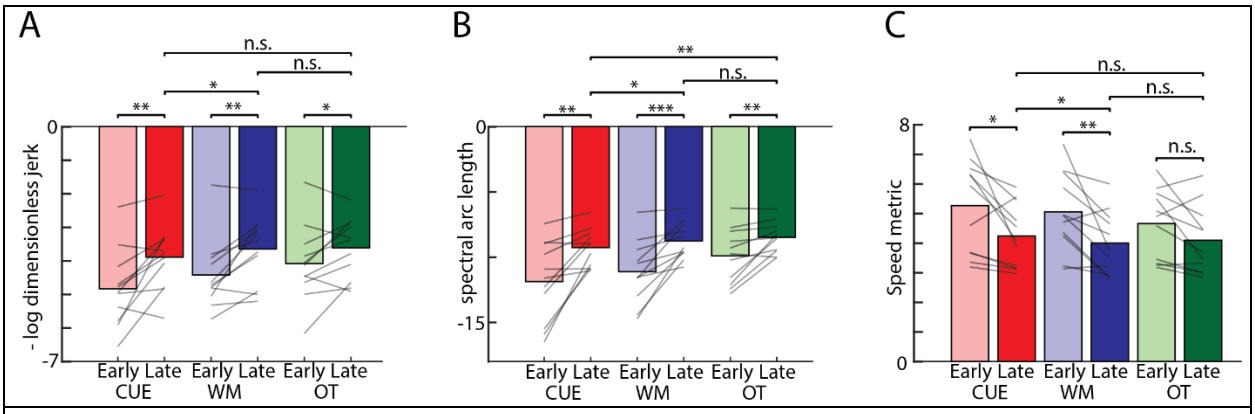

Extended Data Figure 2: Rat's movements become smoother over learning
A-C. Three metrics quantifying movement smoothness, as defined as the continuity or non-intermittency of a movement independent of its amplitude and duration[131], show that smoothness increases throughout learning in all execution modes. Values closer to 0 are defined as smoother. Metrics (see methods) are averaged over trials within each rat (gray lines), and the grand average is plotted (bars). **A.** the negative log dimensionless jerk (derivative of acceleration). **B.** the spectral arc length, or the magnitude of the Fourier spectrum of a movement. **C.** the speed metrics. *P<0.05, **P<0.01, ***P<0.001, Wilcoxon sign rank test.

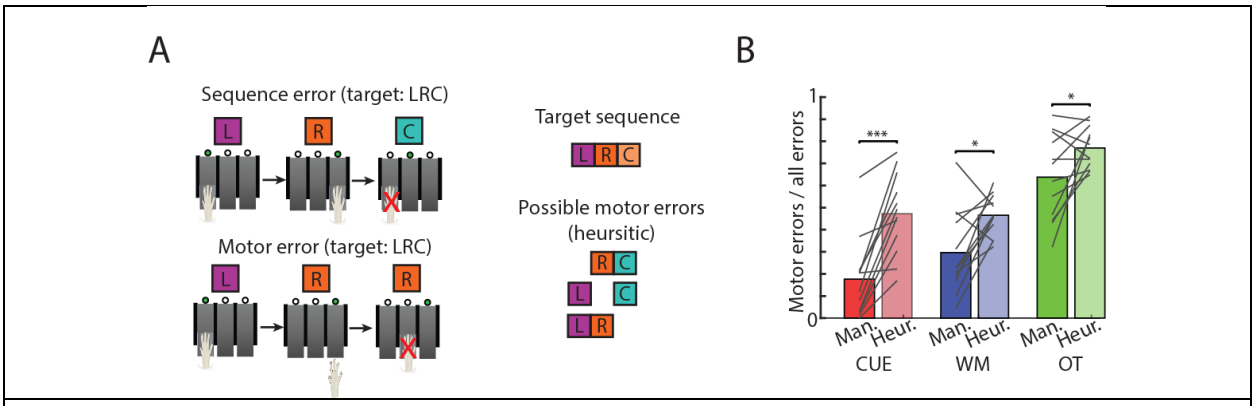

Extended Data Figure 3: Estimating error modes across all trials

A. Rats make two main types of errors: motor errors are when rats orient towards the correct lever but fail to depress it to detection threshold, and continue to perform the correct sequence; sequence errors are when rats orient towards, and press, the incorrect lever. To estimate whether errors were motor errors, we can consider any error sequence with omitted levers. **C.** Motor errors found by the heuristic tend to overestimate the true amount of motor errors, when counted manually. *P<0.05, ***P<0.001, Wilcoxon sign rank test.

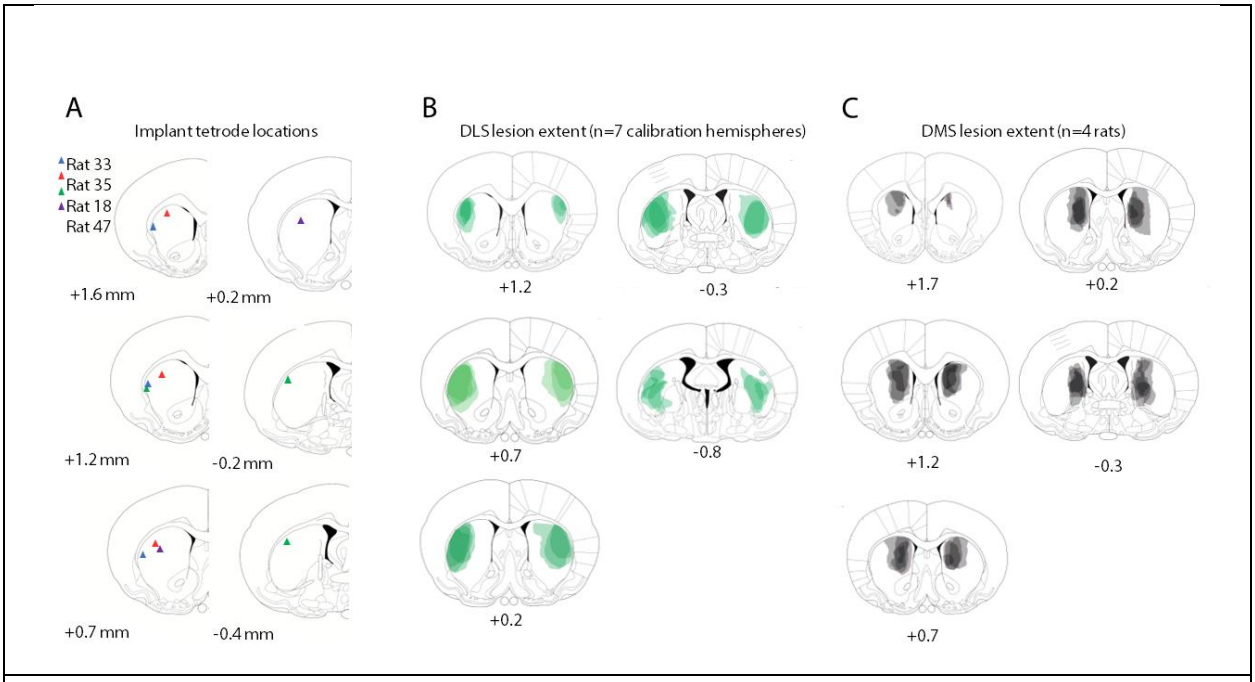

Extended Data Figure 4: Histology of DLS implants, DLS lesions, and DMS lesions

A. Location of recording electrode implantation sites in DLS marked with a colored arrowhead for each of the 4 rats. For some individuals multiple sites are marked, due to individual tetrode bundles spreading during implantation. Coronal slices are labeled from distance relative to bregma. **B.** The extents of 7 calibration hemispheres are marked for the DLS lesion along the anterior-posterior axis of the striatum, and shaded in green. Lesion extent was calibrated to target the motor cortex-recipient region of dorsolateral striatum, as determined from virally-mediated fluorescent labeling in [15]. **C.** Same as B, but eight hemispheres are labeled for DMS lesions. Targeting is based on the prefrontal cortex recipient region of dorsomedial striatum, also from work in [15].

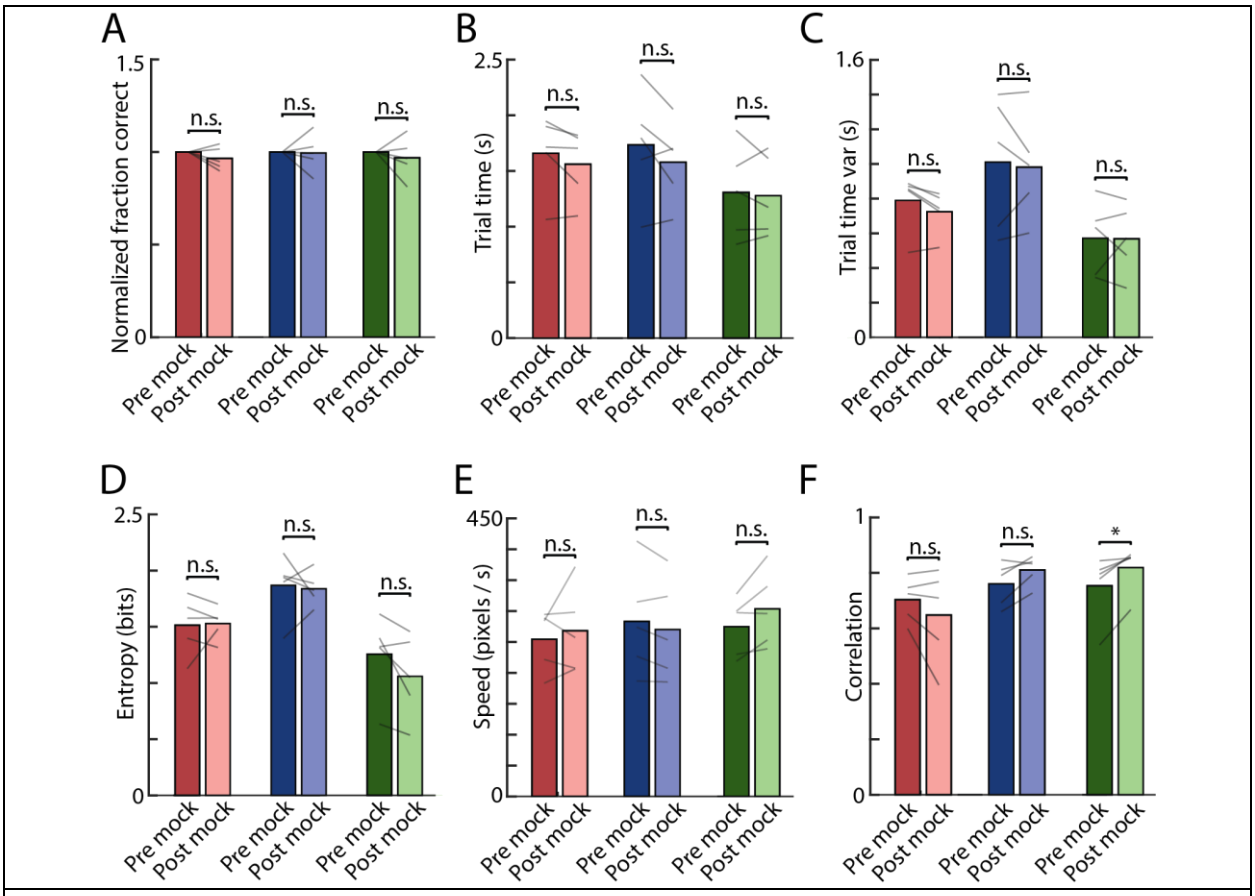

Extended Data Figure 5: Performance on 3-lever task is unaffected by a 7 day mock break in the DLS lesioned cohort

Performance metrics before and after the mock break, in expert animals. Gray lines represent individual rats, bars are averages across rats. **A.** Success rate, **B.** Trial time, **C.** Variance in the trial time, **D.** Entropy, or randomness, of errors, **E.** Average speed during the trial, **F.** Average trial-to-trial correlation. *P<0.05 two-tailed t-test.

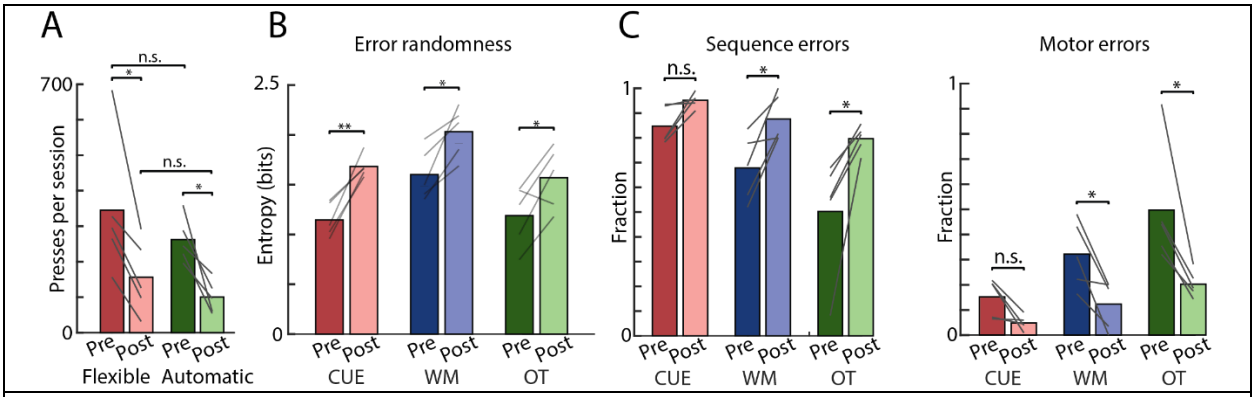

Extended Data Figure 6: Sequence errors increase following the bilateral lesion

A. Lever presses per session for both flexible and automatic sessions decrease following the lesion. **B.** The variability in the sequence mistakes, quantified by calculating the entropy over the distribution of all sequences performed, increases across all three execution modes following the lesion. In the CUE and WM mode, we consider only trials where the target sequence matches the OT sequence. **C.** Changes in the fraction of errors that were motor or sequence (see methods) errors following the lesion. Rats make significantly more sequence errors in the OT and WM mode. *P<0.05, **P<0.01. Two-tailed t-test.

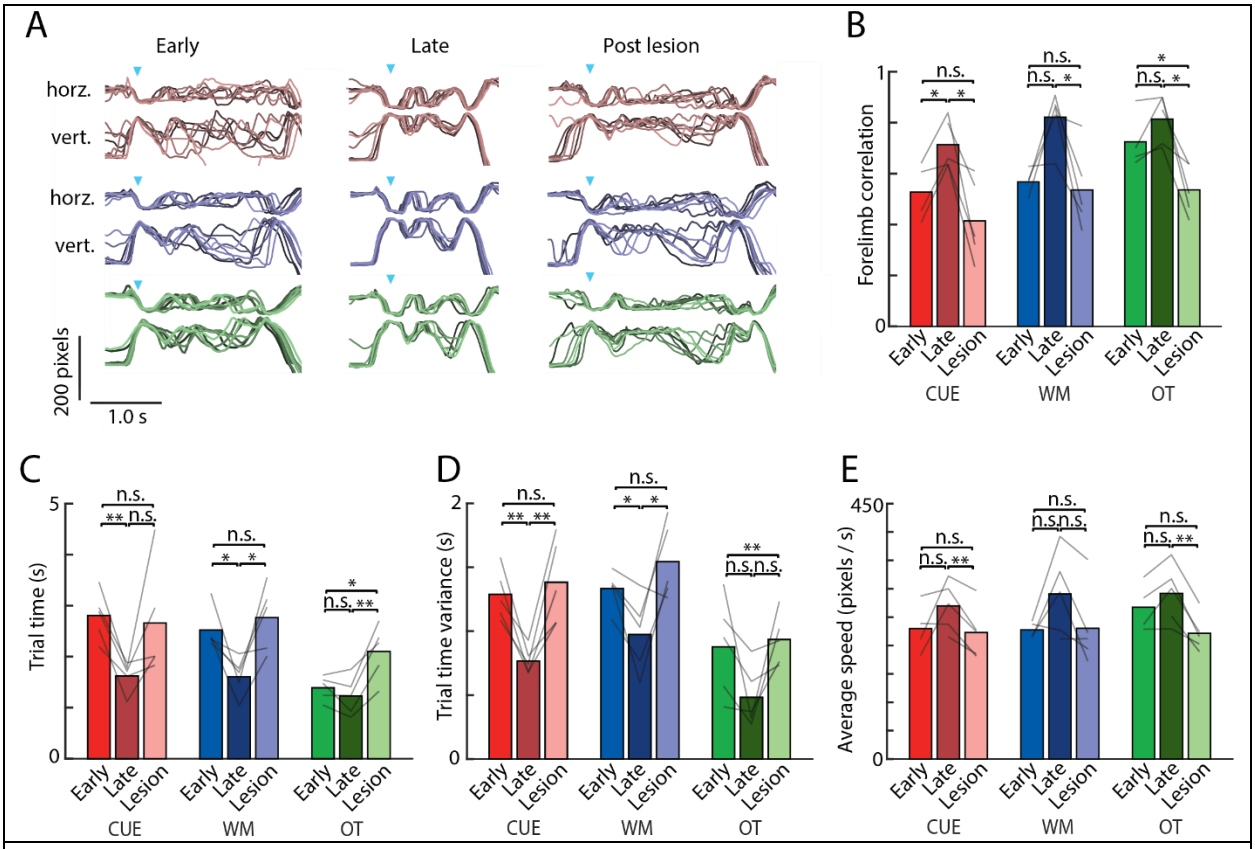

Extended Data Figure 7: Post-lesion kinematics are more similar to early in learning

A. Forelimb kinematics from 8 example trials sampled early in learning, late in learning, and following the bilateral DLS lesion (also see Fig 1e, Fig 5d, and see methods for timing). **B.** Average trial-to-trial correlation for forelimb trajectories of the active paw (both horizontal and vertical) from early in training, compared to late (pre-lesion), and post-lesion, for all execution modes (red=CUE, blue=WM, green=OT). Gray lines are average within rats (n=5 late and lesion, n=4 early, 1 rat was not recorded early in learning) and bars represent average across rats. **C.** Trial time from 1st to 3rd lever press early, late (or pre-lesion), and post-lesion. **D.** Variance in the trial time. E: Average forelimb speed during the trial. *P<0.05, **P<0.01, ***P<0.001.

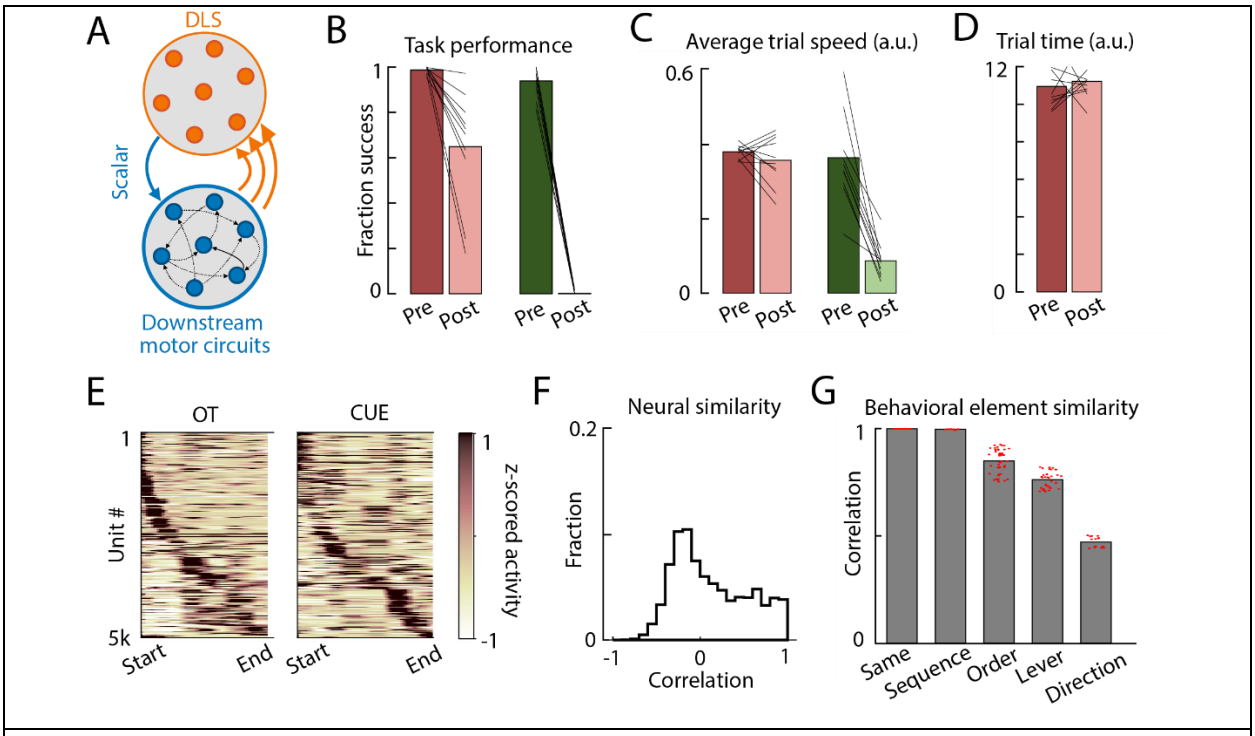

Extended Data Figure 8: A neural network model with scalar DLS outputs fails to learn mode-invariant DLS activity

A. Schematic illustrating architecture of a model variant in which DLS outputs to downstream motor circuits are constrained to be scalar-valued. **B-G:** Replication of analyses in Figure 7c-h, for this model variant. The neural representations are much less similar across modes than in the original model (panels E and F here versus Fig. 7f-g).

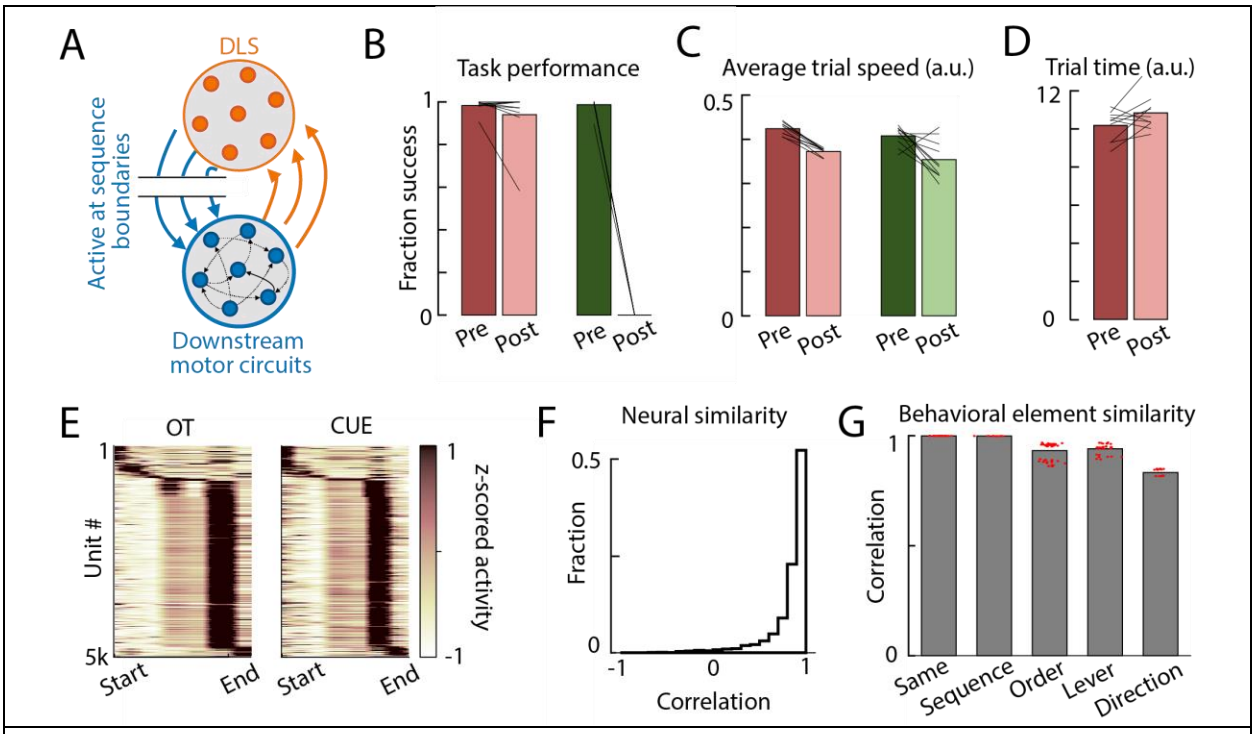

Extended Data Figure 9: A neural network model with action selection signals fails to learn strong kinematic representations

A. Schematic illustrating architecture of a model variant in which DLS outputs to downstream motor circuits are suppressed except at trial initiation and transitions between lever presses. **B-G:** Replication of analyses in Figure 7c-h, for this model variant. The neural representations show much less egocentricity than in the original model (panel G here vs. Fig. 7i).

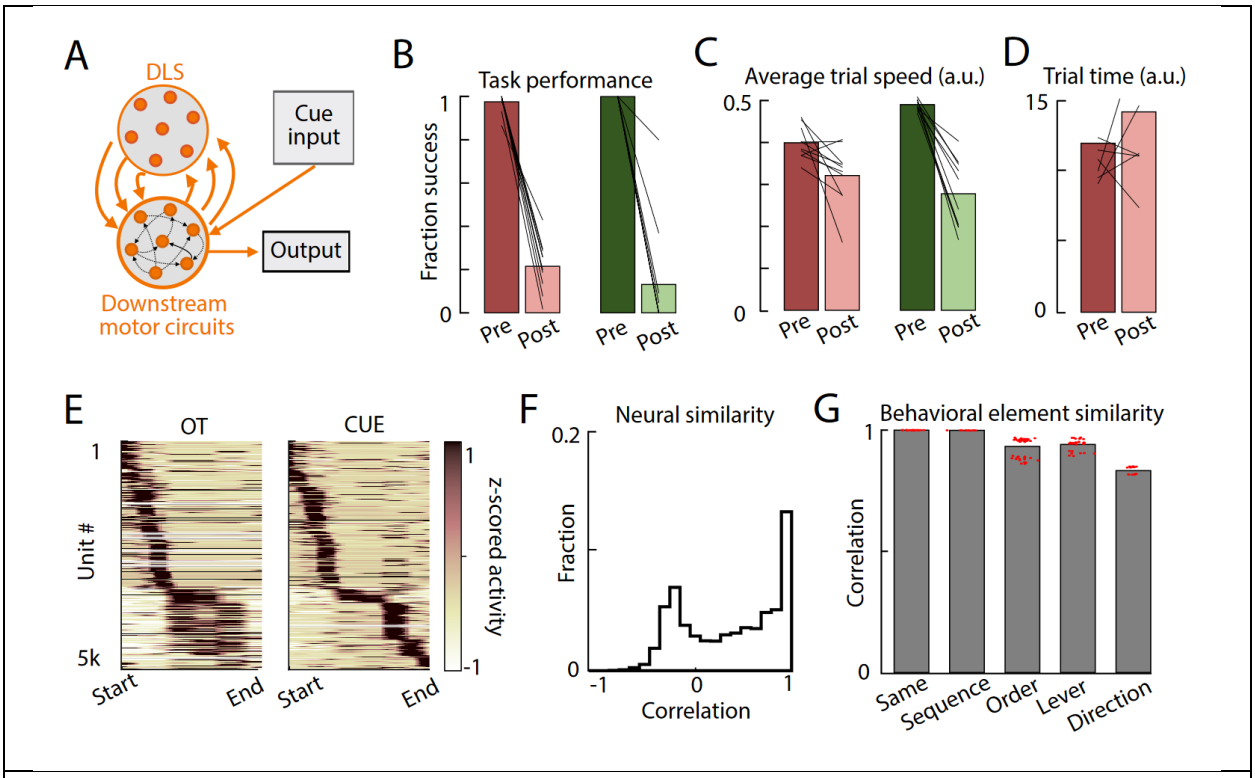

Extended Data Figure 10: A neural network model without pre-trained circuits is not robust to DLS lesions in the flexible mode

A. Schematic illustrating architecture of a model variant in which the entire model is trained on the cued and automatic tasks from scratch, rather than using the strategy of pretraining downstream motor circuits on cued trials first. **B-G:** Replication of analyses in Fig. 7c-h, for this model variant. The resilience of flexible mode performance seen in the original model is lost (panel B here versus Fig. 7c).

Supplementary Info:

Supplementary Video 1:

Three trials of the same motor sequence performed in the CUE, WM, and OT execution mode. Videos are shown first from a top camera, then from a side camera. In the side videos, the kinematics of the active forelimb is tracked and plotted.

Supplementary Video 2:

Trials from the OT mode from an example rat are shown to demonstrate the types of errors we observe. Example trials include five consecutive successful trials, two motor errors that follow a successful trial, and finally a run of sequence errors following motor errors.

Reporting summary:

https://drive.google.com/drive/folders/1THcYMSWYxkvrvjIKDQg388-3uw-J5awY?usp=sharing

References:

1. Schneider, W. & Shiffrin, R. M. Controlled and automatic human information processing: I. Detection, search, and attention. *Psychol. Rev.* **84**, 1–66 (1977).

2. Pashler, H. Dual-task interference in simple tasks: data and theory. *Psychol. Bull.* **116**, 220–244 (1994).

3. Schneider, W. & Chein, J. M. Controlled & automatic processing: behavior, theory, and biological mechanisms. *Cogn. Sci.* **27**, 525–559 (2003).

4. Hardwick, R. M., Forrence, A. D., Krakauer, J. W. & Haith, A. M. Time-dependent competition between goal-directed and habitual response preparation. *Nat. Hum. Behav.* **3**, 1252–1262 (2019).

5. Karni, A. *et al.* The acquisition of skilled motor performance: Fast and slow experience-driven changes in primary motor cortex. *Proc. Natl. Acad. Sci.* **95**, 861–868 (1998).

6. Wiestler, T. & Diedrichsen, J. Skill learning strengthens cortical representations of motor sequences. *eLife* **2**, e00801 (2013).

7. Wymbs, N. F. & Grafton, S. T. The Human Motor System Supports Sequence-Specific Representations over Multiple Training-Dependent Timescales. *Cereb. Cortex N. Y. NY* **25**, 4213–4225 (2015).

8. Ramkumar, P. *et al.* Chunking as the result of an efficiency computation trade-off. *Nat. Commun.* **7**, 12176 (2016).

9. Verwey, W. B., Abrahamse, E. L. & de Kleine, E. Cognitive Processing in New and Practiced Discrete Keying Sequences. *Front. Psychol.* **1**, 32 (2010).

10. Wu, T., Kansaku, K. & Hallett, M. How self-initiated memorized movements become automatic: a functional MRI study. *J. Neurophysiol.* **91**, 1690–1698 (2004).

11. Ashby, F. G., Turner, B. O. & Horvitz, J. C. Cortical and basal ganglia contributions to habit learning and automaticity. *Trends Cogn. Sci.* **14**, 208–215 (2010).

12. Haith, A. M. & Krakauer, J. W. The multiple effects of practice: skill, habit and reduced cognitive load. *Curr. Opin. Behav. Sci.* **20**, 196–201 (2018).

13. Hélie, S. & Cousineau, D. The cognitive neuroscience of automaticity: Behavioral and brain signatures. in *Advances in cognitive and behavioral sciences* 141–159 (Nova Science Publishers, 2014).

14. Hikosaka, O. *et al.* Parallel neural networks for learning sequential procedures. *Trends Neurosci.* **22**, 464–471 (1999).

15. Dhawale, A. K., Wolff, S. B. E., Ko, R. & Ölveczky, B. P. The basal ganglia control the detailed kinematics of learned motor skills. *Nat. Neurosci.* **24**, 1256–1269 (2021).

16. Kawai, R. *et al.* Motor cortex is required for learning but not for executing a motor skill. *Neuron* **86**, 800–812 (2015).

17. Wolff, S. B. E., Ko, R. & Ölveczky, B. P. Distinct roles for motor cortical and thalamic inputs to striatum during motor skill learning and execution. *Sci. Adv.* **8**, eabk0231 (2022).

18. Doyon, J. *et al.* Contributions of the basal ganglia and functionally related brain structures to motor learning. *Behav. Brain Res.* **199**, 61–75 (2009).

19. Isoda, M. & Hikosaka, O. Switching from automatic to controlled action by monkey medial frontal cortex. *Nat. Neurosci.* **10**, 240–248 (2007).

20. Kim, H. F. & Hikosaka, O. Parallel basal ganglia circuits for voluntary and automatic behaviour to reach rewards. *Brain* **138**, 1776–1800 (2015).

21. Lehéricy, S. *et al.* Distinct basal ganglia territories are engaged in early and advanced motor sequence learning. *Proc. Natl. Acad. Sci.* **102**, 12566–12571 (2005).

22. Matsuzaka, Y., Picard, N. & Strick, P. L. Skill representation in the primary motor cortex after long-term practice. *J. Neurophysiol.* **97**, 1819–1832 (2007).

23. Picard, N., Matsuzaka, Y. & Strick, P. L. Extended practice of a motor skill is associated with reduced metabolic activity in M1. *Nat. Neurosci.* **16**, 1340–1347 (2013).

24. Redgrave, P. *et al.* Goal-directed and habitual control in the basal ganglia: implications for Parkinson's disease. *Nat. Rev. Neurosci.* **11**, 760–772 (2010).

25. Berlot, E., Popp, N. J. & Diedrichsen, J. In search of the engram, 2017. *Curr. Opin. Behav. Sci.* **20**, 56–60 (2018).

26. Diedrichsen, J. & Kornysheva, K. Motor skill learning between selection and execution. *Trends Cogn. Sci.* **19**, 227–233 (2015).

27. Ohbayashi, M. The Roles of the Cortical Motor Areas in Sequential Movements. *Front. Behav. Neurosci.* **15**, 97 (2021).

28. Lanciego, J. L., Luquin, N. & Obeso, J. A. Functional Neuroanatomy of the Basal Ganglia. *Cold Spring Harb. Perspect. Med.* **2**, a009621 (2012).

29. Geddes, C. E., Li, H. & Jin, X. Optogenetic Editing Reveals the Hierarchical Organization of Learned Action Sequences. *Cell* **174**, 32-43.e15 (2018).

30. Miyachi, S., Hikosaka, O. & Lu, X. Differential activation of monkey striatal neurons in the early and late stages of procedural learning. *Exp. Brain Res.* **146**, 122–126 (2002).

31. Miyachi, S., Hikosaka, O., Miyashita, K., Karádi, Z. & Rand, M. Differential roles of monkey striatum in learning of sequential hand movement. *Exp. Brain Res. Exp. Hirnforsch. Expérimentation Cérébrale* **115**, 1–5 (1997).

32. Yin, H. H. The Sensorimotor Striatum Is Necessary for Serial Order Learning. *J. Neurosci.* **30**, 14719–14723 (2010).

33. Sharpe, M. J. *et al.* An Integrated Model of Action Selection: Distinct Modes of Cortical Control of Striatal Decision Making. *Annu. Rev. Psychol.* **70**, 53–76 (2019).

34. Kim, H. F. & Hikosaka, O. Distinct basal ganglia circuits controlling behaviors guided by flexible and stable values. *Neuron* **79**, 1001–1010 (2013).

35. Pinsard, B. *et al.* Consolidation alters motor sequence-specific distributed representations. *eLife* **8**, e39324 (2019).

36. Seidler, R. D. *et al.* Neural correlates of encoding and expression in implicit sequence learning. *Exp. Brain Res.* **165**, 114–124 (2005).

37. Hikosaka, O., Kim, H. F., Yasuda, M. & Yamamoto, S. Basal Ganglia Circuits for Reward Value–Guided Behavior. *Annu. Rev. Neurosci.* **37**, 289–306 (2014).

38. Graybiel, A. M. & Grafton, S. T. The striatum: where skills and habits meet. *Cold Spring Harb. Perspect. Biol.* **7**, a021691 (2015).

39. Houk, J. c *et al.* Action selection and refinement in subcortical loops through basal ganglia and cerebellum. *Philos. Trans. R. Soc. B Biol. Sci.* **362**, 1573–1583 (2007).

40. Andersen, K. W., Madsen, K. H. & Siebner, H. R. Discrete finger sequences are widely represented in human striatum. *Sci. Rep.* **10**, 13189 (2020).

41. Kermadi, I. & Joseph, J. P. Activity in the caudate nucleus of monkey during spatial sequencing. *J. Neurophysiol.* **74**, 911–933 (1995).

42. Desmurget, M. & Turner, R. S. Motor Sequences and the Basal Ganglia: Kinematics, Not Habits. *J. Neurosci.* **30**, 7685–7690 (2010).

43. Mushiake, H., Inase, M. & Tanji, J. Neuronal activity in the primate premotor, supplementary, and precentral motor cortex during visually guided and internally determined sequential movements. *J. Neurophysiol.* **66**, 705–718 (1991).

44. Mushiake, H. & Strick, P. L. Pallidal neuron activity during sequential arm movements. *J. Neurophysiol.* **74**, 2754–2758 (1995).

45. Menon, V., Anagnoson, R. T., Glover, G. H. & Pfefferbaum, A. Basal ganglia involvement in memory-guided movement sequencing. *Neuroreport* **11**, 3641–3645 (2000).

46. Barnes, T. D., Kubota, Y., Hu, D., Jin, D. Z. & Graybiel, A. M. Activity of striatal neurons reflects dynamic encoding and recoding of procedural memories. *Nature* **437**, 1158–1161 (2005).

47. Jin, X., Tecuapetla, F. & Costa, R. M. Basal ganglia subcircuits distinctively encode the parsing and concatenation of action sequences. *Nat. Neurosci.* **17**, 423–430 (2014).

48. Jin, X. & Costa, R. M. Start/Stop Signals Emerge in Nigrostriatal Circuits during Sequence Learning. *Nature* **466**, 457–462 (2010).

49. Jog, M. S., Kubota, Y., Connolly, C. I., Hillegaart, V. & Graybiel, A. M. Building neural representations of habits. *Science* **286**, 1745–1749 (1999).

50. Martiros, N., Burgess, A. A. & Graybiel, A. M. Inversely Active Striatal Projection Neurons and Interneurons Selectively Delimit Useful Behavioral Sequences. *Curr. Biol. CB* **28**, 560-573.e5 (2018).

51. Jin, X. & Costa, R. M. Shaping Action Sequences in Basal Ganglia Circuits. *Curr. Opin. Neurobiol.* **33**, 188–196 (2015).

52. Rothwell, P. E. *et al.* Input- and Output-Specific Regulation of Serial Order Performance by Corticostriatal Circuits. *Neuron* **88**, 345–356 (2015).

53. Jurado-Parras, M.-T. *et al.* The Dorsal Striatum Energizes Motor Routines. *Curr. Biol.* **30**, 4362-4372.e6 (2020).

54. Park, J., Coddington, L. T. & Dudman, J. T. Basal Ganglia Circuits for Action Specification. *Annu. Rev. Neurosci.* **43**, 485–507 (2020).

55. Pimentel-Farfan, A. K., Báez-Cordero, A. S., Peña-Rangel, T. M. & Rueda-Orozco, P. E. Cortico-striatal circuits for bilaterally coordinated movements. *Sci. Adv.* **8**, eabk2241 (2022).

56. Sales-Carbonell, C. *et al.* No discrete start/stop signals in the dorsal striatum of mice performing a learned action. *Curr. Biol. CB* **28**, 3044-3055.e5 (2018).

57. Abrahamse, E. L., Ruitenberg, M. F. L., de Kleine, E. & Verwey, W. B. Control of automated behavior: insights from the discrete sequence production task. *Front. Hum. Neurosci.* **7**, (2013).

58. Braun, S. & Hauber, W. The dorsomedial striatum mediates flexible choice behavior in spatial tasks. *Behav. Brain Res.* **220**, 288–293 (2011).

59. Castañé, A., Theobald, D. E. H. & Robbins, T. W. Selective lesions of the dorsomedial striatum impair serial spatial reversal learning in rats. *Behav. Brain Res.* **210**, 74–83 (2010).

60. Cox, J. & Witten, I. B. Striatal circuits for reward learning and decision-making. *Nat. Rev. Neurosci.* **20**, 482–494 (2019).

61. Ragozzino, M. E., Ragozzino, K. E., Mizumori, S. J. Y. & Kesner, R. P. Role of the Dorsomedial Striatum in Behavioral Flexibility for Response and Visual Cue Discrimination Learning. *Behav. Neurosci.* **116**, 105–115 (2002).

62. Yin, H. H. & Knowlton, B. J. The role of the basal ganglia in habit formation. *Nat. Rev. Neurosci.* **7**, 464–476 (2006).

63. Tanji, J. Sequential Organization of Multiple Movements: Involvement of Cortical Motor Areas. *Annu. Rev. Neurosci.* **24**, 631–651 (2001).

64. Du, Y., Krakauer, J. W. & Haith, A. M. The relationship between habits and motor skills in humans. *Trends Cogn. Sci.* **0**, (2022).

65. Kondapavulur, S. *et al.* Transition from predictable to variable motor cortex and striatal ensemble patterning during behavioral exploration. *Nat. Commun.* **13**, 2450 (2022).

66. Adams, C. D. & Dickinson, A. Instrumental Responding following Reinforcer Devaluation. *Q. J. Exp. Psychol. Sect. B* **33**, 109–121 (1981).

67. Derusso, A. L. *et al.* Instrumental uncertainty as a determinant of behavior under interval schedules of reinforcement. *Front. Integr. Neurosci.* **4**, 17 (2010).

68. Dickinson, A., Nicholas, D. J. & Adams, C. D. The effect of the instrumental training contingency on susceptibility to reinforcer devaluation. *Q. J. Exp. Psychol. B* **35**, 35–51 (1983).

69. Urcelay, G. P. & Jonkman, S. Delayed rewards facilitate habit formation. *J. Exp. Psychol. Anim. Learn. Cogn.* **45**, 413–421 (2019).

70. Macdonald, G. E. & de Toledo, L. Partial reinforcement effects and type of reward. *Learn. Motiv.* **5**, 288–298 (1974).

71. Shillinglaw, J. E., Everitt, I. K. & Robinson, D. L. Assessing behavioral control across reinforcer solutions on a fixed-ratio schedule of reinforcement in rats. *Alcohol* **48**, 337–344 (2014).

72. Vandaele, Y., Pribut, H. J. & Janak, P. H. Lever Insertion as a Salient Stimulus Promoting Insensitivity to Outcome Devaluation. *Front. Integr. Neurosci.* **11**, 23 (2017).

73. Ma, L., Hyman, J. M., Phillips, A. G. & Seamans, J. K. Tracking Progress toward a Goal in Corticostriatal Ensembles. *J. Neurosci.* **34**, 2244–2253 (2014).

74. Erlich, J. C., Bialek, M. & Brody, C. D. A cortical substrate for memory-guided orienting in the rat. *Neuron* **72**, 330–343 (2011).

75. Kopec, C. D., Erlich, J. C., Brunton, B. W., Deisseroth, K. & Brody, C. D. Cortical and Subcortical Contributions to Short-Term Memory for Orienting Movements. *Neuron* **88**, 367–377 (2015).

76. Turner, K. M., Svegborn, A., Langguth, M., McKenzie, C. & Robbins, T. W. Opposing Roles of the Dorsolateral and Dorsomedial Striatum in the Acquisition of Skilled Action Sequencing in Rats. *J. Neurosci.* **42**, 2039–2051 (2022).

77. Ohbayashi, M., Picard, N. & Strick, P. L. Inactivation of the Dorsal Premotor Area Disrupts Internally Generated, But Not Visually Guided, Sequential Movements. *J. Neurosci.* **36**, 1971–1976 (2016).

78. Shima, K. & Tanji, J. Neuronal activity in the supplementary and presupplementary motor areas for temporal organization of multiple movements. *J. Neurophysiol.* **84**, 2148–2160 (2000).

79. Tanji, J. & Shima, K. Role for supplementary motor area cells in planning several movements ahead. *Nature* **371**, 413–416 (1994).

80. Insafutdinov, E., Pishchulin, L., Andres, B., Andriluka, M. & Schiele, B. DeeperCut: A Deeper, Stronger, and Faster Multi-person Pose Estimation Model. in *Computer Vision – ECCV 2016* (eds. Leibe, B., Matas, J., Sebe, N. & Welling, M.) 34–50 (Springer International Publishing, 2016). doi:10.1007/978-3-319-46466-4_3.

81. Mathis, A. *et al.* DeepLabCut: markerless pose estimation of user-defined body parts with deep learning. *Nat. Neurosci.* **21**, 1281–1289 (2018).

82. Dhawale, A. K., Smith, M. A. & Ölveczky, B. P. The Role of Variability in Motor Learning. *Annu. Rev. Neurosci.* **40**, 479–498 (2017).

83. Rueda-Orozco, P. E. & Robbe, D. The striatum multiplexes contextual and kinematic information to constrain motor habits execution. *Nat. Neurosci.* **18**, 453–460 (2015).

84. Popp, N. J., Yokoi, A., Gribble, P. L. & Diedrichsen, J. The effect of instruction on motor skill learning. *J. Neurophysiol.* **124**, 1449–1457 (2020).

85. Karni, A. *et al.* Functional MRI evidence for adult motor cortex plasticity during motor skill learning. *Nature* **377**, 155–158 (1995).

86. Thorn, C. A., Atallah, H., Howe, M. & Graybiel, A. M. Differential Dynamics of Activity Changes in Dorsolateral and Dorsomedial Striatal Loops During Learning. *Neuron* **66**, 781–795 (2010).

87. Markowitz, J. E. *et al.* The Striatum Organizes 3D Behavior via Moment-to-Moment Action Selection. *Cell* **174**, 44-58.e17 (2018).

88. Ma, L., Hyman, J. M., Lindsay, A. J., Phillips, A. G. & Seamans, J. K. Differences in the emergent coding properties of cortical and striatal ensembles. *Nat. Neurosci.* **17**, 1100–1106 (2014).

89. Bailey, K. R. & Mair, R. G. The Role of Striatum in Initiation and Execution of Learned Action Sequences in Rats. *J. Neurosci.* **26**, 1016–1025 (2006).

90. Dudman, J. T. & Krakauer, J. W. The basal ganglia: from motor commands to the control of vigor. *Curr. Opin. Neurobiol.* **37**, 158–166 (2016).

91. Mello, G. B. M., Soares, S. & Paton, J. J. A scalable population code for time in the striatum. *Curr. Biol. CB* **25**, 1113–1122 (2015).

92. Toso, A., Reinartz, S., Pulecchi, F. & Diamond, M. E. Time coding in rat dorsolateral striatum. *Neuron* **109**, 3663-3673.e6 (2021).

93. Gouvêa, T. S., Monteiro, T., Soares, S., Atallah, B. V. & Paton, J. J. Ongoing behavior predicts perceptual report of interval duration. *Front. Neurorobotics* **8**, 10 (2014).

94. Kock, R. D., Gladhill, K. A., Ali, M. N., Joiner, W. M. & Wiener, M. How movements shape the perception of time. *Trends Cogn. Sci.* **25**, 950–963 (2021).

95. Safaie, M. *et al.* Turning the body into a clock: Accurate timing is facilitated by simple stereotyped interactions with the environment. *Proc. Natl. Acad. Sci.* **117**, 13084–13093 (2020).

96. Robbe, D. To move or to sense? Incorporating somatosensory representation into striatal functions. *Curr. Opin. Neurobiol.* **52**, 123–130 (2018).

97. Ye, Z. *et al.* The Role of the Subthalamic Nucleus in Sequential Working Memory in De Novo Parkinson's Disease. *Mov. Disord.* **36**, 87–95 (2021).

98. Burleigh-Jacobs, A., Horak, F. B., Nutt, J. G. & Obeso, J. A. Step initiation in Parkinson's disease: influence of levodopa and external sensory triggers. *Mov. Disord. Off. J. Mov. Disord. Soc.* **12**, 206–215 (1997).

99. Siegert, R. J., Harper, D. N., Cameron, F. B. & Abernethy, D. Self-initiated versus externally cued reaction times in Parkinson's disease. *J. Clin. Exp. Neuropsychol.* **24**, 146–153 (2002).

100. Lewis, S. J. G., Dove, A., Robbins, T. W., Barker, R. A. & Owen, A. M. Striatal contributions to working memory: a functional magnetic resonance imaging study in humans. *Eur. J. Neurosci.* **19**, 755–760 (2004).

101. Alexander, G. E., DeLong, M. R. & Strick, P. L. Parallel organization of functionally segregated circuits linking basal ganglia and cortex. *Annu. Rev. Neurosci.* **9**, 357–381 (1986).

102. Hunnicutt, B. J. *et al.* A comprehensive excitatory input map of the striatum reveals novel functional organization. *eLife* **5**, e19103 (2016).

103. Vandaele, Y. *et al.* Distinct recruitment of dorsomedial and dorsolateral striatum erodes with extended training. *eLife* **8**, e49536 (2019).

104. Burke, D. A., Rotstein, H. G. & Alvarez, V. A. Striatal Local Circuitry: A New Framework for Lateral Inhibition. *Neuron* **96**, 267–284 (2017).

105. Tunstall, M. J., Oorschot, D. E., Kean, A. & Wickens, J. R. Inhibitory Interactions Between Spiny Projection Neurons in the Rat Striatum. *J. Neurophysiol.* **88**, 1263–1269 (2002).

106. Shadmehr, R. & Ahmed, A. A. *Vigor: Neuroeconomics of Movement Control*. (MIT Press, 2020).

107. Lu, X. & Ashe, J. Anticipatory activity in primary motor cortex codes memorized movement sequences. *Neuron* **45**, 967–973 (2005).

108. Stephenson-Jones, M., Samuelsson, E., Ericsson, J., Robertson, B. & Grillner, S. Evolutionary conservation of the basal ganglia as a common vertebrate mechanism for action selection. *Curr. Biol. CB* **21**, 1081–1091 (2011).

109. Verwey, W. B. Buffer loading and chunking in sequential keypressing. *J. Exp. Psychol. Hum. Percept. Perform.* **22**, 544–562 (1996).

110. Graybiel, A. M. The basal ganglia and chunking of action repertoires. *Neurobiol. Learn. Mem.* **70**, 119–136 (1998).

111. Lashley, K. S. The problem of serial order in behavior. in *Cerebral mechanisms in behavior; the Hixon Symposium* 112–146 (Wiley, 1951).

112. Carelli, R. M., Wolske, M. & West, M. O. Loss of lever press-related firing of rat striatal forelimb neurons after repeated sessions in a lever pressing task. *J. Neurosci.* **17**, 1804–1814 (1997).

113. Tang, C., Pawlak, A. P., Prokopenko, V. & West, M. O. Changes in activity of the striatum during formation of a motor habit. *Eur. J. Neurosci.* **25**, 1212–1227 (2007).

114. Balleine, B. W. Neural bases of food-seeking: affect, arousal and reward in corticostriatolimbic circuits. *Physiol. Behav.* **86**, 717–730 (2005).

115. Dickinson, A. & Weiskrantz, L. Actions and habits: the development of behavioural autonomy. *Philos. Trans. R. Soc. Lond. B Biol. Sci.* **308**, 67–78 (1985).

116. Dolan, R. J. & Dayan, P. Goals and Habits in the Brain. *Neuron* **80**, 312–325 (2013).

117. de Wit, S. *et al.* Shifting the balance between goals and habits: Five failures in experimental habit induction. *J. Exp. Psychol. Gen.* **147**, 1043–1065 (2018).

118. Cushman, F. & Morris, A. Habitual control of goal selection in humans. *Proc. Natl. Acad. Sci.* **112**, 13817–13822 (2015).

119. Simon, D. A. & Daw, N. D. Dual-System Learning Models and Drugs of Abuse. in *Computational Neuroscience of Drug Addiction (eds. Gutkin, B. & Ahmed, S. H.)* 145–161 (Springer, 2012). doi:10.1007/978-1-4614-0751-5_5.

120. Aldridge, J. W., Berridge, K. C. & Rosen, A. R. Basal ganglia neural mechanisms of natural movement sequences. *Can. J. Physiol. Pharmacol.* **82**, 732–739 (2004).

121. Levy, R., Friedman, H. R., Davachi, L. & Goldman-Rakic, P. S. Differential activation of the caudate nucleus in primates performing spatial and nonspatial working memory tasks. *J. Neurosci. Off. J. Soc. Neurosci.* **17**, 3870–3882 (1997).

122. Akhlaghpour, H. *et al.* Dissociated sequential activity and stimulus encoding in the dorsomedial striatum during spatial working memory. *eLife* **5**, e19507 (2016).

123. Spencer, R. C., Klein, R. M. & Berridge, C. W. Psychostimulants Act Within the Prefrontal Cortex to Improve Cognitive Function. *Biol. Psychiatry* **72**, 221–227 (2012).

124. Ma, J. *et al.* Impaired serial ordering in nondemented patients with mild Parkinson's disease. *PLoS ONE* **13**, e0197489 (2018).

125. Rogers, M. A., Phillips, J. G., Bradshaw, J. L., Iansek, R. & Jones, D. Provision of external cues and movement sequencing in Parkinson's disease. *Motor Control* **2**, 125–132 (1998).

126. Ashe, J., Lungu, O. V., Basford, A. T. & Lu, X. Cortical control of motor sequences. *Curr. Opin. Neurobiol.* **16**, 213–221 (2006).

127. Yokoi, A. & Diedrichsen, J. Neural Organization of Hierarchical Motor Sequence Representations in the Human Neocortex. *Neuron* **103**, 1178-1190.e7 (2019).

128. Murray, J. M. & Escola, G. S. Remembrance of things practiced with fast and slow learning in cortical and subcortical pathways. *Nat. Commun.* **11**, 6441 (2020).

129. Guo, J.-Z. *et al.* Cortex commands the performance of skilled movement. *eLife* **4**, e10774 (2015).

130. Poddar, R., Kawai, R. & Ölveczky, B. P. A Fully Automated High-Throughput Training System for Rodents. *PLoS ONE* **8**, e83171 (2013).

131. Balasubramanian, S., Melendez-Calderon, A., Roby-Brami, A. & Burdet, E. On the analysis of movement smoothness. *J. NeuroEngineering Rehabil.* **12**, 112 (2015).

132. Beck, Y. *et al.* SPARC: a new approach to quantifying gait smoothness in patients with Parkinson's disease. *J. NeuroEngineering Rehabil.* **15**, 49 (2018).

133. Gulde, P. & Hermsdörfer, J. Smoothness Metrics in Complex Movement Tasks. *Front. Neurol.* **9**, (2018).

134. Refai, M. I. M. *et al.* Smoothness metrics for reaching performance after stroke. Part 1: which one to choose? *J. NeuroEngineering Rehabil.* **18**, NA-NA (2021).

135. Dhawale, A. K. *et al.* Automated long-term recording and analysis of neural activity in behaving animals. *eLife* **6**, e27702 (2017).

136. Paxinos, G. *The Rat Brain in Stereotaxic Coordinates*. (Academic Press, 1998).

137. Masís, J. *et al.* A micro-CT-based method for quantitative brain lesion characterization and electrode localization. *Sci. Rep.* **8**, 5184 (2018).

138. Beal, M., Kowall, N., Swartz, K., Ferrante, R. & Martin, J. Systemic approaches to modifying quinolinic acid striatal lesions in rats. *J. Neurosci.* **8**, 3901–3908 (1988).

139. Feng, Q. *et al.* Specific Reactions of Different Striatal Neuron Types in Morphology Induced by Quinolinic Acid in Rats. *PLOS ONE* **9**, e91512 (2014).

140. Harris, K. D., Henze, D. A., Csicsvari, J., Hirase, H. & Buzsáki, G. Accuracy of tetrode spike separation as determined by simultaneous intracellular and extracellular measurements. *J. Neurophysiol.* **84**, 401–414 (2000).

141. Schmitzer-Torbert, N., Jackson, J., Henze, D., Harris, K. & Redish, A. D. Quantitative measures of cluster quality for use in extracellular recordings. *Neuroscience* **131**, 1–11 (2005).

142. Hill, D. N., Mehta, S. B. & Kleinfeld, D. Quality Metrics to Accompany Spike Sorting of Extracellular Signals. *J. Neurosci.* **31**, 8699–8705 (2011).

143. Lewicki, M. S. A review of methods for spike sorting: the detection and classification of neural action potentials. *Netw. Bristol Engl.* **9**, R53-78 (1998).

144. He, K., Zhang, X., Ren, S. & Sun, J. Delving Deep into Rectifiers: Surpassing Human-Level Performance on ImageNet Classification. in *2015 IEEE International Conference on Computer Vision (ICCV)* 1026–1034 (2015). doi:10.1109/ICCV.2015.123.